



Data Article

Petrography descriptions and U-Pb zircon datasets from the Archean Pavas Block, Precambrian of Uruguay



Henri Masquelin^{a,*}, Tahar Aifa^b, Fernando Scaglia^c,
Miguel A.S. Basei^d

^a Instituto de Ciencias Geológicas, Facultad de Ciencias – UdelaR, Iguá 4225 p12 ala sur, 11400 Montevideo, Uruguay

^b Univ. Rennes, CNRS, Géosciences Rennes – UMR6118, Campus Beaulieu, 35042 Rennes, France

^c Post-graduate Course, PEDECIBA Geosciences, Uruguay

^d Centro de Pesquisas Geocronológicas, Universidade de São Paulo, Brazil

ARTICLE INFO

Article history:

Received 7 May 2021

Accepted 26 May 2021

Available online 29 May 2021

Keywords:

Gneiss complex

Nico Pérez Terrane

Zircon texture

Orosirian

U-Pb geochronology

ABSTRACT

This database is a geological and geochronological compilation made to study a small Archean/Paleoproterozoic block located in the centre of the Precambrian rock exposition of Uruguay. Petrographic and field outcrops data supporting the samples from which the zircons for textural analysis and U-Pb dating (LA-ICP-MS) come are presented at first with their descriptions. The first table (1) contains the new U-Pb isotopic data. The second table (2) presents a correlation of textures from different zircon samples. The last table (3) contains an inventory of different U-Pb ages found in antecedents. All these data are associated with the paper entitled: “The Archean Pavas Block in Uruguay: extension and tectonic evolution based on LA-ICP-MS U-Pb ages and airborne geophysics”.

© 2021 Published by Elsevier Inc.

This is an open access article under the CC BY license

(<http://creativecommons.org/licenses/by/4.0/>)

DOI of original article: [10.1016/j.jsames.2021.103364](https://doi.org/10.1016/j.jsames.2021.103364)

* Corresponding author.

E-mail address: emasquelin@fcien.edu.uy (H. Masquelin).

Social media:  (H. Masquelin)

<https://doi.org/10.1016/j.dib.2021.107179>

2352-3409/© 2021 Published by Elsevier Inc. This is an open access article under the CC BY license

(<http://creativecommons.org/licenses/by/4.0/>)

Specifications Table

| | |
|--------------------------------|---|
| Subject | Earth and Planetary Sciences, Geology. |
| Specific subject area | Geochronology, U-Pb dating system. |
| Type of data | Figures with descriptive text and tables. |
| How data were acquired | Petrographic microscope, binocular microscope, SEM cathodoluminescence, IsoplotR software (Vermeesch 2018), QGIS (GNU) software, Oasis-Montaj 8.3.0© (Geosoft Inc.). Laser ablation ICP-MS mass spectrometry using the Excimer laser of ArF gas (193 nm) coupled to the Neptune™ High-Resolution Multi-collector ICP-MS at the Geochronological Laboratory of the Geosciences Institute from the University of São Paulo (Brazil). |
| Data format | Raw (Photos and U-Pb data), analysed, processed, and filtered. |
| Parameters for data collection | Representative sample collection for the La China Complex and the Campanero Gneisses for U-Pb geochronology. Petrographic thin sections were prepared. Zircons mounted in epoxy resin were described. |
| Description of data collection | Petrography and U-Pb zircon analyses of the granitic – gneisses and migmatites of the Pavas Block, a segment composed of pre-Neoproterozoic basement rocks westward the Neoproterozoic Dom Feliciano Belt. |
| Data source location | Zapicán, Route 40, Penitente, El Soldado; Lavalleja Department; Uruguay. All the cartographic coordinates in the text are in the reference system EPSG 32721 (UTM wgs84 21S). Zapicán (Lat. -33.40887, Long. -54.90875; Lat. -33.55428; Long. -54.89335) Route 40 (Lat. -33.74979, Long. -55.09939; Lat. -33.75518, -54.99020) Penitente (Lat. -34.33662, Long. -55.10061) El Soldado (Lat. -34.14855, Long. -55.26246) Primary data sources of data in antecedent are shown in the last column of Table III (see Reference list). |
| Data accessibility | Data are available within the article and in the repository. Repository name: Mendeley Data identification number: http://dx.doi.org/10.17632/7hk685mzjn.1 Direct URL to data: http://dx.doi.org/10.17632/7hk685mzjn.1 |
| Related research article | H. Masquelin, T. Aïfa, F. Scaglia, M.A.S. Basei, The Archean Pavas Block in Uruguay: extension and tectonic evolution based on LA-ICP-MS U-Pb ages and airborne geophysics, J. South American Earth Sciences. In Press. |

Value of the Data

- U-Pb isotopic data in zircon confirm the presence in Uruguay of Archean metamorphic crystallisation rocks without subsequent recycling.
- These data can be helpful to establish correlations between accreted terranes within the Brasiliano amalgamation.
- They can be used together with other U-Pb and Lu-Hf isotopic data to refine model ages and understand the origin of the protoliths.
- The exploitation of these U-Pb isotopic analyses varies between 94% and 38% depending on each sample since many spots have a high content of common Pb.
- Petrographic data of the La China Complex encompasses more than the samples that were dated because it attempts to show the geodiversity within this gneissic complex to construct a more detailed geological map.

1. Data Description

1.1. Petrographic data

This petrographic description primarily represents the dated samples but not exclusively. All these rock samples come from a migmatite complex and range from highly plastically deformed to slightly affected by strain. The most abundant rocks are orthogneisses with amphibio-

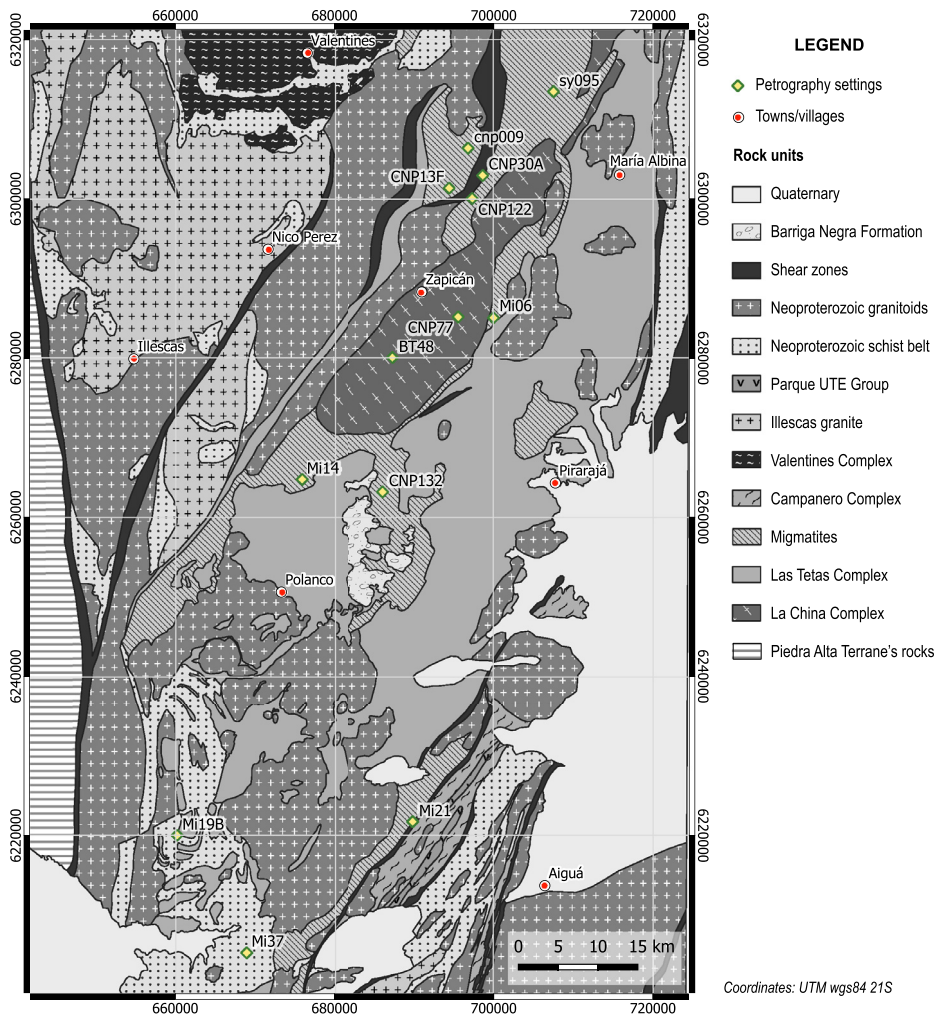


Fig. 1. Geological location of the petrographic and zircon isotopic samples in the Pavas Block (central Uruguay).

lite boudins or schlieren. These rocks usually show pegmatite injections. Hydrothermally altered granitoids include grey metatonalites that enclose some xenoliths of retrogressed mafic rocks. The gneissic layering (SL) and mineral lineation (Lm) was added to each sample when available. The gneisses generally show amphibolite facies metamorphic mineral assemblages. However, different minerals and microstructures indicate widespread hydrothermalism in the greenschist facies. Interspersed banded felsic gneisses and amphibolites are shown. The studied outcrops are showing in the map (Fig. 1).

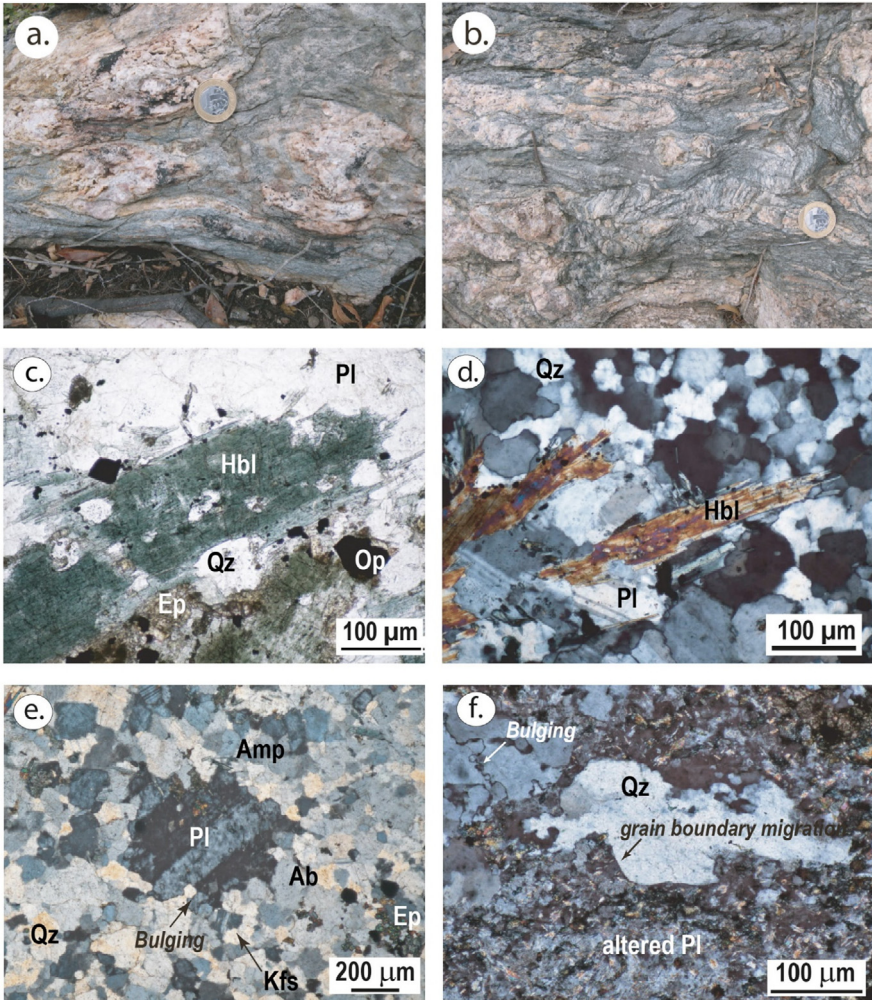


Fig. 2. a) Amphibole-bearing orthogneiss with amphibolite blocks (CNP13F) (a to d), containing b) Ep+Hbl+Pl mineral assemblage; c) Polygonal texture and grain-boundary migration recrystallisation on Qz; d) Epidote net texture; e) Mus+Ep+Pl orthogneiss (CNP77) (e to h), with f) Ep-Mus hydrothermal veins; g) Saussuritic plagioclase, and epidote veins; h) Detailed mineral inclusions within the saussurite; Mineral abbreviations follow the criteria of Whitney and Evans [5].

1.2. Petrographic description of dated samples

1.2.1. Sample CNP13F

Amphibole-bearing orthogneiss with sharp-angled boudins of amphibolite (Fig. 2a; coord.: $x = 681875$; $y = 6251285$). The rotated boudins allow deducing a dextral kinematic sense ($Lm = 20/190$; $SL = 50/45$). In the thin section, the orthogneiss texture is granoblastic lobate equigranular (~100–200 μm grain-sized) (Fig. 2b). It is composed of brown to green amphibole (tschermakite, hornblende), Ca-plagioclase, quartz, epidote (Fig. 2c). Accessories include zircon, opaques, and apatite. Epidote developed a skeletal or net texture around polygonal plagioclase grains (Fig. 2d). There are domains almost entirely composed of quartz which contain hornblende and plagioclase. The “chessboard” pattern is common on quartz sub-fabric [1].

1.2.2. Sample CNP77

Flat-lying composite layered rock (Fig. 2e; coord.: $x=695628$; $y=6285289$) which separates into (i) a coarse-grained white augen gneiss and (ii) a biotite-bearing mylonite (SL: 150/18; Lm: 5/230). The coarse-grained rock dominates in the thin section. Epidote-muscovite-bearing quartz veins crosscut the layering both discordant and concordantly (Fig. 2f). The texture is porphyroblastic heterogranular. Crystal-size is c. 500 μm on average. The coarse-grained rock (i) is composed of quartz (35%), poikiloblastic saussuritic Ca-plagioclase (50%), microcline, muscovite, and epidote in veins (Fig. 2g). A detailed overview shows minute grains of well-crystallised zoisite and muscovite (Fig. 2h). Carlsbad/albite twinned oligoclase (An₂₄) is present. Accessory minerals are pale-brown biotite, opaque minerals, titanite, apatite and zircon. Dynamic recrystallisation of quartz is due to diffusion-assisted grain-boundary migration [1]. Patchy-perthite feldspar is present in the porphyroclasts.

1.2.3. Sample Mi21

Fine-grained amphibole-bearing orthogneiss crosscut by Kfs-rich granitic veins (coord.: $x = 689924$; $y = 6221711$) (Fig. 3a). A low-temperature mylonitization/cataclasis (Sm: 33/30) crosscut the high-temperature layering (Fig. 3b). The texture is grano-nematoblastic heterogranular. The mineralogy is Ca-plagioclase (40%), quartz (30%), hornblende (10%) and epidote (3%). Accessory minerals include zircon, apatite, and opaque minerals. Hornblende is dark-to-pale green coloured (Fig. 3c). There are fibrous amphiboles in contact with fine-grained quartz-feldspar granoblastic domains (Fig. 3d). The metamorphic peak assemblage includes hornblende and ternary feldspar (dark), a relic of the pre-mylonitic mineral assemblage (Fig. 3e). Quartz rarely shows lobate contacts against plagioclase due to high-temperature grain boundary migration, but the main deformation mechanism is bulging and recovery [1] (Fig. 3f). Hornblende presents zonation, epidote coronas and opaque inclusions.

1.2.4. Sample Mi30

Dark green layered migmatite injected by folded Kfs-rich granitic (leucosome) veins (coord.: $x = 674723$; $y = 6198889$). The layering (SL: 260/70) becomes partially into a mylonitic foliation, and the grain size is due to mylonitization (Fig. 4a). Leucosome veins are deformed (Fig. 4b). The main texture is granoblastic inequigranular (Fig. 4c). The mineralogy is composed of quartz (35%), Ca-plagioclase (saussurite) (35%), K-feldspar (albite, microcline) (25%), biotite (3%), epidote (0.5%), chlorite (0.2%) and sericite (0.5%). Accessory minerals are opaques, apatite, zircon, and allanite. Ca-plagioclase shows a myriad of sericite-epidote inclusions (Fig. 4d). There are two kinds of biotite: (i) oriented selvage of pale-green biotite and (ii) brown biotite aggregates associated with the accessory minerals. Bulging and recovery are the mechanisms of grain-boundary migration recrystallisation in quartz. The allanite is in isolated grains and has at least 500 μm in size (Fig. 4e). Zircons usually are associated with sericite-epidote aggregates (Fig. 4f).

1.2.5. Sample Mi14

The primary rock is a medium-grained grey orthogneiss, crosscut by a K-feldspar-rich pegmatite (coord.: $x=676057$; $y=6263943$) (Fig. 5a). The texture of the grey orthogneiss is granoblastic inequigranular and lobate. The mineralogy contains plagioclase (An₄₃) (45%), quartz (30%), K-feldspar (20%), and very few biotite. Accessory minerals are apatite, zircon, and muscovite.

1.2.6. Sample Mi19B

Composite-layered mylonitic granitoid (coord.: $x=660189$, $y=6219998$). The "granitic" layers produced a ribbon-quartz, Kfs-rich, porphyroclastic mylonite (Fig. 5b). The mylonitic granite crosscut a fine-grained granoblastic metapsammite and a lepidoblastic mica-schist with biotite muscovite and tourmaline. The mylonitic foliation (Sm: 330/26) was affected by upright cylindrical folding, whose axes parallel the stretching lineation (Lm: 20/195). The thin section reveals a fine-grained muscovite-rich quartz-feldspathic matrix, crosscut by 1–2 mm thick anastomosed quartz ribbons (Fig. 5c). Lobate quartz-grains in these ribbons are medium-grained, although

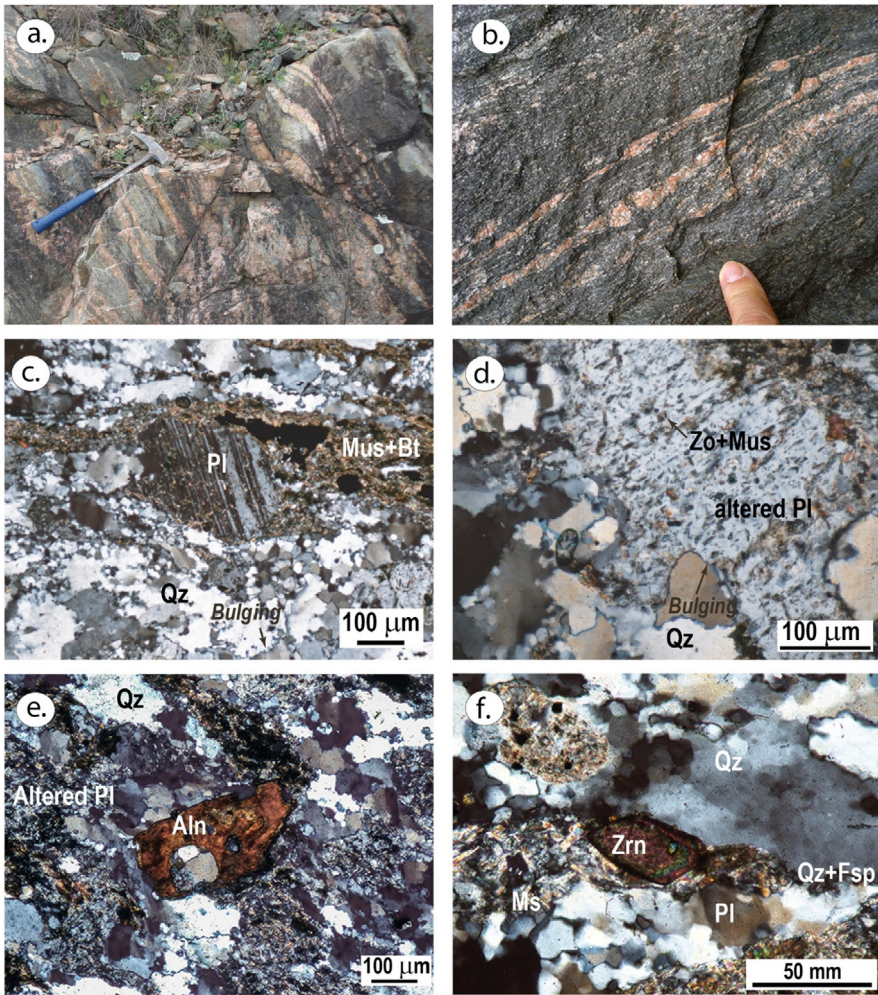


Fig. 3. Hbl-bearing orthogneisses (sample Mi21): a) Amphibole-bearing orthogneiss with pegmatite injections; b) incipient cataclastic deformation on the same outcrop; c) Hornblende associated with epidote and opaque minerals; d) Hbl-Pl-bearing gneiss (crossed Nicols); e) Older Ca-plagioclase surrounded by recrystallised matrix; f) Remnant of older quartz-boundary surrounded by low-temperature recrystallised matrix (crossed Nicols).

developing an incipient bulging and undulose extinction. The inequigranular matrix has a granoblastic polygonal texture, and the biotite is decussate (Fig. 5d). This matrix surrounds large plagioclase grains (An₂₅). Muscovite is often secondary, but there are also large kinked muscovites. We also found biotite selvages parallel to the layering.

1.3. Petrographic description of supplementary samples

1.3.1. Sample CNP122

Epidote-bearing tremolite schist represents a set of mafic rocks interspersed within the felsic orthogneisses of La China Complex (coord.: x=697392; y=6300113). In the field, they usually appear as amphibolite blocks or lenses (Fig. 5e). These mafic rocks have different degrees

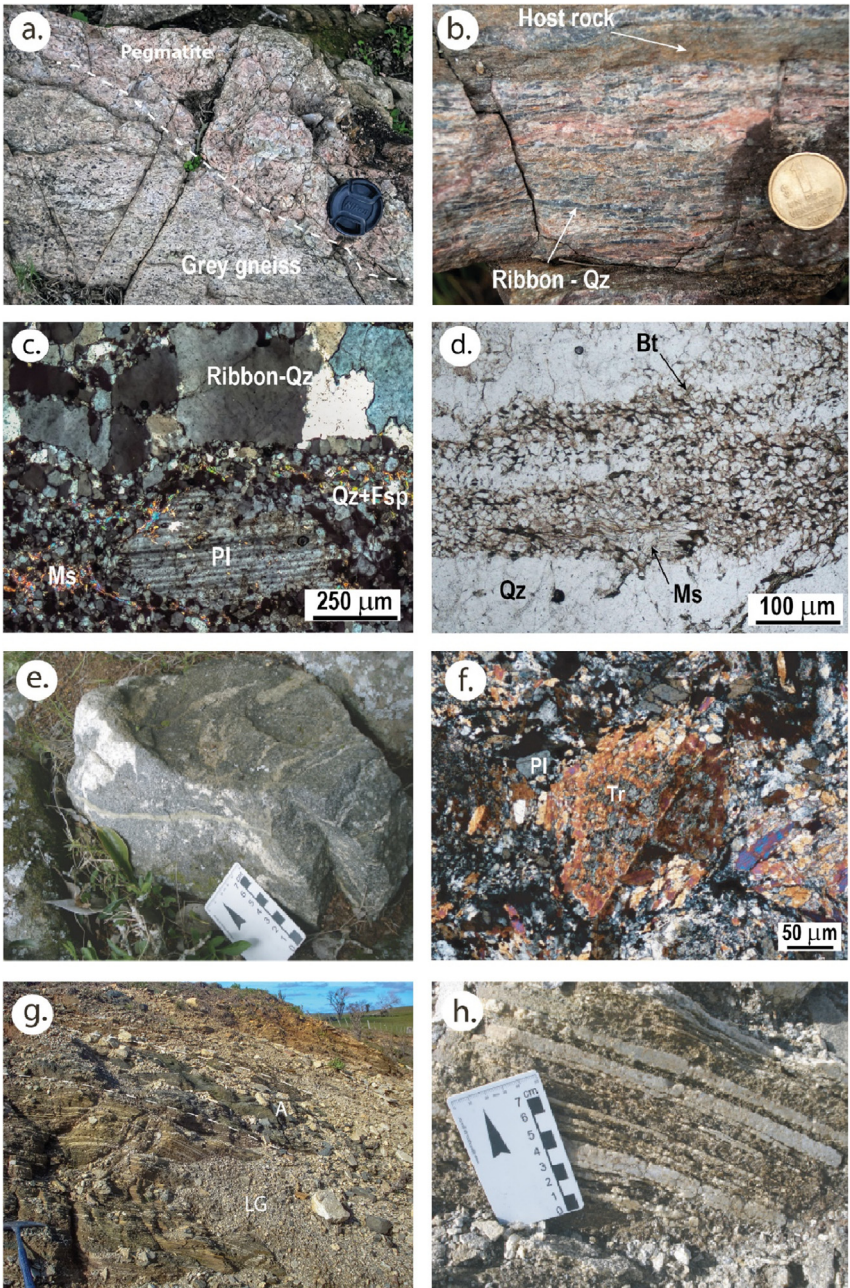


Fig. 4. Biotite-bearing migmatite orthogneiss (sample Mi30): a) Composite layered migmatite showing concordant granitic veins; b) Diffuse segregation of in-situ leucosome; c) main texture of the rock showing fine-grained Bt + Ms layers and plagioclase grains in a quartz-feldspathic matrix; d) Altered saussuritic plagioclase with epidote-sericite inclusions; e) Isolated crystal of allanite in a matrix with complete alteration of feldspar; f) Subhedral zircon in the quartz-feldspathic matrix.

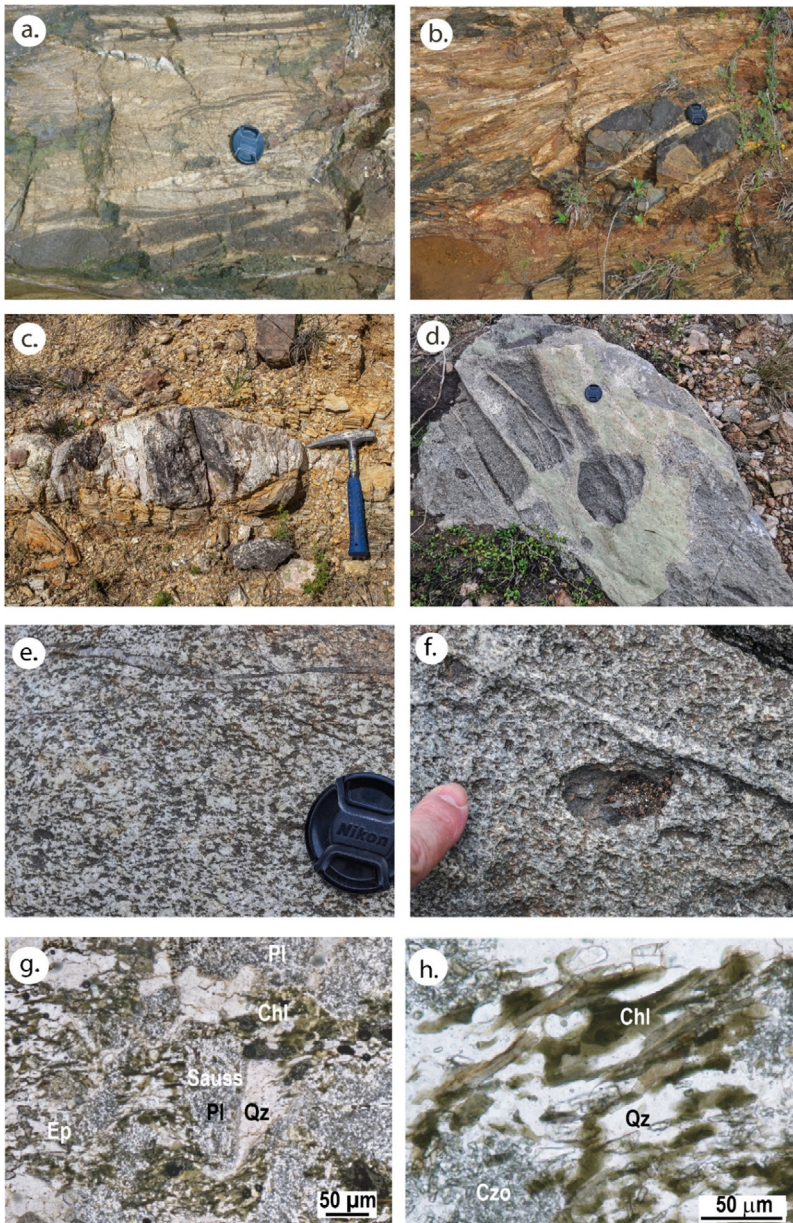


Fig. 5. Different orthogneisses and mafic rocks: a) Felsic orthogneiss crosscut by a K-feldspar pegmatite (Mi14); b) Mylonitic K-feldspar granitoid within biotite-tourmaline bearing schist (Mi19b); c) Detailed texture showing a folded ribbon-quartz (vein) crosscutting a quartz-feldspathic granoblastic matrix with decussate biotite and larger kinked muscovite (centre below; crossed Nicols); d) Idem, granoblastic matrix (natural light); e) Amphibolite boudin (CNP009); f) Twinned tremolite showing symplectite with Ab in retrograde mafic schist (CNP122); g) Low-angle cm-width gneissic banding (LG), showing the alternation between felsic layered gneisses and amphibolites (A)(CNP30A); h) Detail of gneiss layering.

of retrograde metamorphism. The symplectite between magnetite and tremolite represents the dominant texture. The tremolite texture is an aggregate of fibrous poikiloblastic bundles (> 2 mm). Basal sections show the trace of twins on (001) face (Fig. 5f). Some altered plagioclases (saussurite), quartz and opaques filled up the interstitial space among tremolite crystals.

1.3.2. Sample CNP30A

Straight layered fine-grained gneiss interspersed with amphibolite (coord. UTM84 21S: x = 698689; y = 6302989) (Fig. 5g). The mylonitic foliation (Sm: 70/27) is parallel to the centimetre-width layering (Fig. 5h) and contain a stretching lineation (Lm: 21/272). This banding represents the relicts of a wide high-strain zone with relative flat-lying foliation, which limited the Pavas and the Cerro Chato "terranes" (i.e., Sierra de Sosa high strain zone). The layering was produced at relatively high temperature and persisted despite many rocks in the region passed to retrograde conditions. Layered amphibolites are likely the same as those found in straight and short "boudins" or lenses but in the different structural setting. The thin section was unable here due to the alteration of the rock.

1.3.3. Sample CNP132

Fine-grained layered migmatitic gneiss containing biotite *schlieren* (Fig. 6a) (coord. UTM84 21S: x = 686153; y = 6263198). The gneissic layering (SL: 144/25) contains some amphibolite boudins unaffected by anatexis (Fig. 6b). Some white pegmatites are showing pinch-and-swell and crosscut the migmatitic gneiss (Fig. 6c). We select one pegmatite dyke for zircon sampling. Texture in quartz- feldspathic domains is granoblastic heterogranular with large patchy perthite K-feldspar. Muscovite is present as well as accessory minerals, e.g., zircon and apatite. The rock did not bring enough zircons of good quality (low common Pb) to produce an acceptable Pb-loss Discordia age.

1.3.4. Sample BT48

Medium grained gray granitoid crosscut by veinlets (Fig. 6d; coord. UTM wgs84 21S: x = 687409; y = 6280088). Mafic enclaves appear disseminated (Fig. 6f). The texture is granular hypidiomorphic and composed of poikilitic Ca-Plagioclase (saussurite) in the process of albitisation, microcline, quartz, chlorite, green biotite, zoisite, apatite, calcite, and sericite (Fig. 6g). Ca-plagioclase is subhedral and shows Ab and Carlsbad twins. Although the deformation is weak, the rock developed a domianial cleavage of its secondary hydrothermal mineralogy of chlorite and epidote (Fig. 6h). Fine-grained zoisite and sericite within plagioclase are alteration minerals. Hydrothermal albite is twinned and limpid. Brown biotite is magmatic and arranged around feldspar and quartz. Pressure shadows are often present around euhedral feldspar grains. Quartz texture is granoblastic and lobate.

1.3.5. Sample SY95A

Amphibole-biotite coarse-grained mesocratic granodiorite or monzogranite (coord. UTM wgs84 21S: x= 706825; y=6315572). The hand sample is a porphyroblastic orthogneiss (SL: 265/10; Lm: 10/238) (Fig. 7a). A mafic dyke crosscut the main granodiorite. The dyke transformed into a medium-grained amphibolite (D: 50/65) (Fig. 7b); there is a strong mineral lineation on it (Lm: 5/253) (Fig. 7c). The texture of the granodiorite is granular hypidiomorphic but slightly deformed. K-feldspar phenocrysts reach 3-4 cm and are surrounded by hornblende-biotite aggregates (Fig. 7d). The mineralogy is microcline, plagioclase, hornblende, quartz, biotite (brown), titanite (3%), apatite, opaque minerals, epidote, zircon, and monazite. Biotite and amphibole are intergrowing with titanite, apatite and monazite (Fig. 7e). The amphibolite shows a granoblastic texture composed of hornblende and plagioclase (Fig. 7f).

1.3.6. Sample Mi06

Low-angle composite mylonitic rock (SL: 085/20; Lm: 5/170) (Fig. 8a; coord.: x=699986; y=6285192). The outcrop comprises (i) a white augen gneiss and (ii) a fine-grained biotite mylonite. The protolith of the augen gneiss may be a pegmatite injected into the mylonite. Its

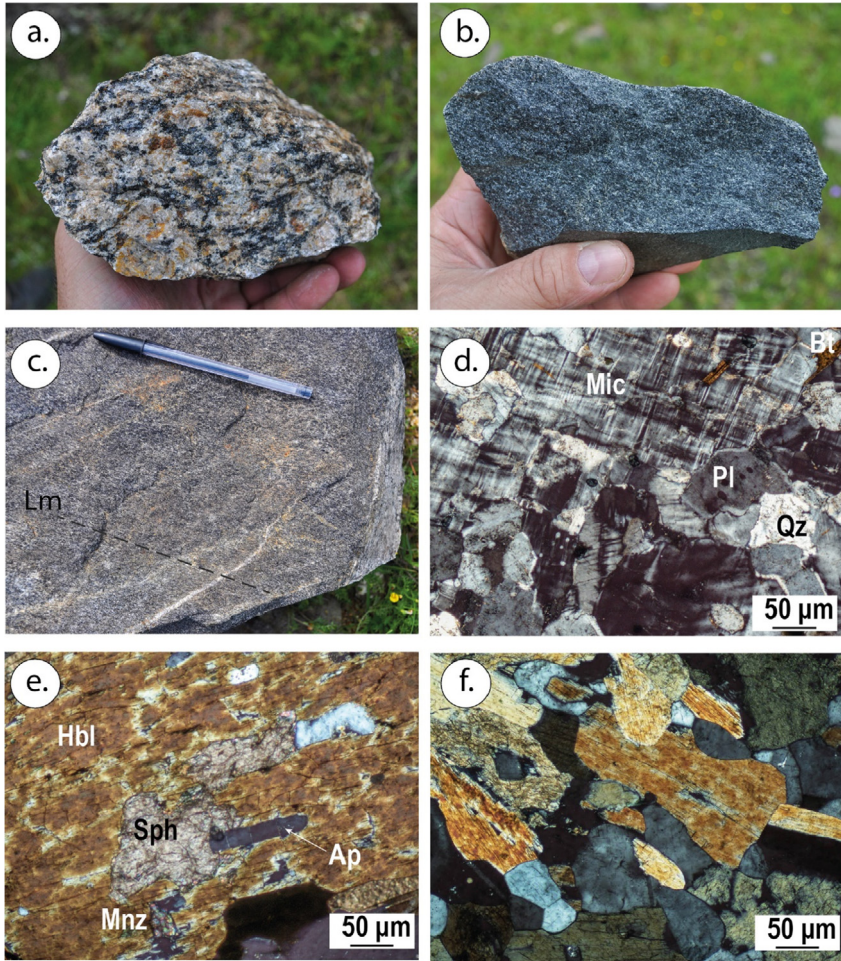


Fig. 6. a) Granitic gneiss with biotite schlieren (CNP132) (a to c) containing b) amphibolite boudins, c) “white” pegmatite dyke, concordant with the layering; d) Foliated grey orthogneiss (BT48) (d to g) with e) Magmatic texture observed in the field; f) Mafic enclaves; g) Domianial cleavage around saussuritic altered plagioclase (natural light). g) Chl-Ep bearing cleavage.

mineralogy includes K-feldspar, plagioclase (An₅₀), quartz, muscovite, opaque minerals, biotite, apatite, and zircon. The mylonite has a fine-grained equigranular granoblastic texture. Its minerals are plagioclase, ternary feldspar, quartz, reddish biotite, apatite, and zircon. Porphyroclasts have a recrystallisation mantle (Fig. 8b). The pressure shadows show an aggregate of fine-grained feldspars (Fig. 8c, d). Porphyroclasts have an antiperthitic nucleus (Pl+Mic) (Fig. 8e, f). Recrystallisation could have occurred by rotation of subgrains within the augen themselves (Fig. 8g). Metamorphic plagioclase exhibits muscovite and quartz inclusions. Albite twins are fuzzy, irregular, and sinuous. Quartz appears in different forms: (i) black quartz fishes (Fig. 8c, d), (ii) ribbons (Fig. 8b, h) and (iii) equidimensional grains. Quartz ribbons and muscovite aggregates cover the porphyroclasts (Fig. 8i). Porphyroclasts define a blurred sigma-delta system, but the shear direction is ambiguous (Fig. 8a, b, f).

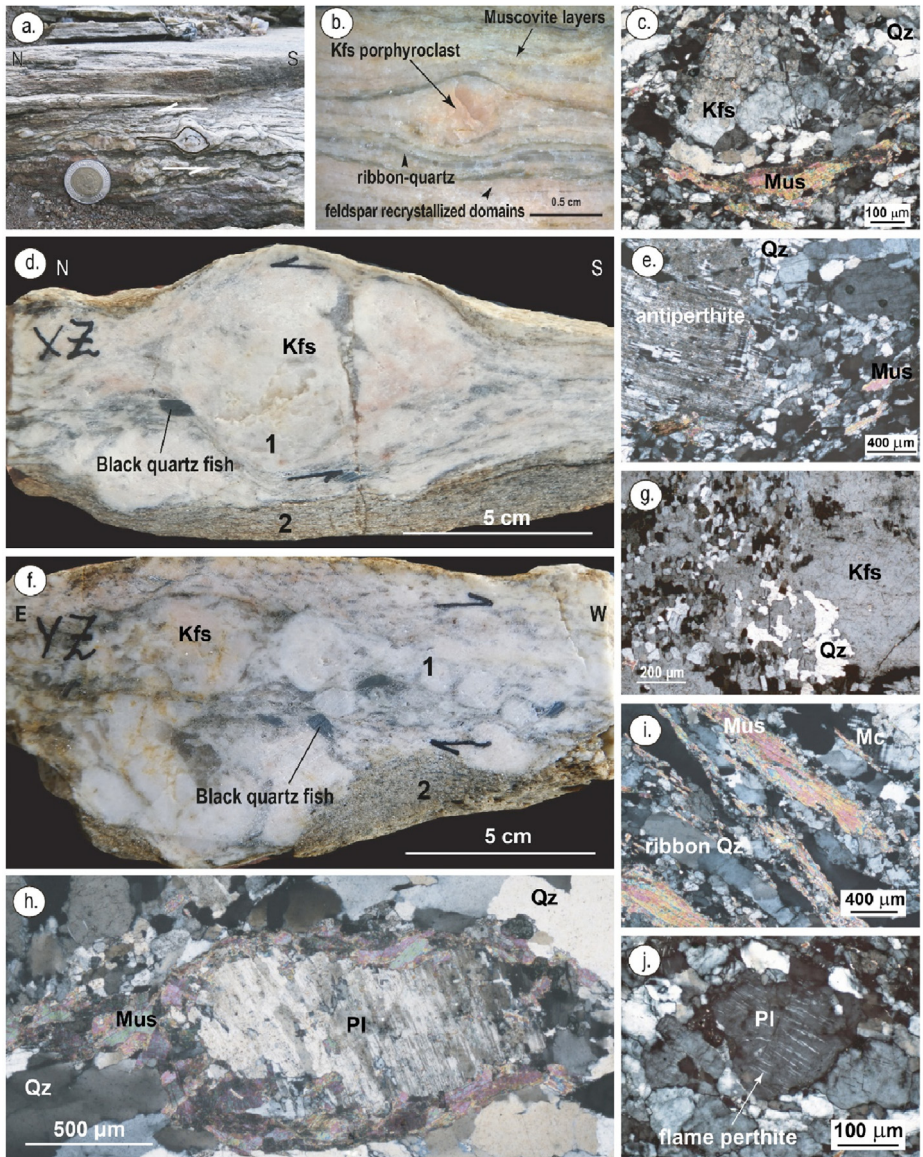


Fig. 7. a) Amphibole-biotite granodiorite (SY95) (a to f); b) medium-grained foliated amphibolite from a mafic dyke; c) stretching lineation of the amphibolite; d) texture of the granodiorite with recrystallised microcline phenocrysts, plagioclase, and quartz; e) Hbl containing titanite, apatite and monazite inclusions; f) granoblastic texture of the amphibolite (crossed Nicols).

2. U-Pb Isotopic Data of Zircons

The new U-Pb isotopic data by Laser ablation – ICP – MS are presented in [Table I](#).

The correlation of different textural features between the sample's zircons is presented in [Table II](#). Older U-Pb age references are presented in [Table III](#).

Table 1
LA-ICP-MS U-Pb zircon analytical data. The analytical errors are in the 1σ , but the selected spots for calculations at the 2σ error.

| # | RATIOS | | | | | | | | | | Pb* | Th | U | AGES | | | | | Conc.206/238 vs 207/206 | Interpretation (Ma) | | | | | |
|--|-------------|------------|-------------|------------|-------------|------------|--------------|------------|--------------|------------|------|------|------|------------|-------------|------|------|------------|----------------------------|------------------------|------------|------------|----------------------------------|------------|------------|
| | 207Pb/ 235U | | 206Pb/ 238U | | 238U/ 206Pb | | 207Pb/ 206Pb | | 208Pb/ 206Pb | | | | | 1 σ | Pb* (%) | ppm | Th/U | T206/ 238 | | | T207/ 235 | | 1 σ | 1 σ | |
| | 1 σ | 1 σ | 1 σ | 1 σ | 1 σ | 1 σ | 1 σ | 1 σ | 1 σ | 1 σ | | | | | | | | 1 σ | | | 1 σ | 1 σ | | | 1 σ |
| CNP13F - Layered amphibole - bearing orthogneiss | | | | | | | | | | | | | | | | | | | | | | | | | |
| 30.1 | 23.788 | 0.357 | 0.647 | 0.007 | 1.546 | 0.017 | 0.267 | 0.004 | 0.161 | 0.017 | 0.30 | 22.5 | - | 24.8 | - | 3216 | 27 | 3260 | 14 | 3287 | 24 | 97 | Concordia Age: 3261 \pm 16 | | |
| 34.1 | 22.683 | 0.601 | 0.649 | 0.008 | 1.540 | 0.018 | 0.253 | 0.007 | 0.201 | 0.027 | 0.26 | 55.3 | 22.5 | 58.1 | 0.39 | 3226 | 30 | 3213 | 26 | 3206 | 44 | 100 | | | |
| 25.1 | 23.742 | 0.372 | 0.651 | 0.007 | 1.536 | 0.017 | 0.264 | 0.004 | 0.233 | 0.034 | 0.11 | 18.7 | 16.9 | 18.9 | 0.89 | 3233 | 28 | 3258 | 14 | 3273 | 25 | 98 | | | |
| 26.1 | 22.969 | 0.579 | 0.652 | 0.013 | 1.534 | 0.031 | 0.256 | 0.007 | 0.255 | 0.047 | 0.71 | 6.2 | - | 7 | - | 3236 | 54 | 3226 | 31 | 3219 | 52 | 100 | | | |
| 12.1 | 24.380 | 0.471 | 0.652 | 0.006 | 1.534 | 0.015 | 0.271 | 0.006 | 0.122 | 0.006 | 0.41 | 45.9 | - | 50.2 | - | 3236 | 25 | 3284 | 19 | 3313 | 32 | 97 | | | |
| 35.1 | 23.808 | 0.511 | 0.655 | 0.005 | 1.527 | 0.013 | 0.264 | 0.006 | 0.166 | 0.004 | 0.34 | 41.5 | 35 | 46.6 | 0.75 | 3247 | 21 | 3261 | 21 | 3269 | 33 | 99 | | | |
| 27.1 | 23.361 | 0.378 | 0.658 | 0.008 | 1.521 | 0.018 | 0.258 | 0.004 | 0.207 | 0.022 | 0.22 | 12.8 | 7.5 | 13.4 | 0.56 | 3258 | 30 | 3242 | 15 | 3233 | 26 | 100 | | | |
| 2.1 | 23.631 | 0.447 | 0.662 | 0.006 | 1.512 | 0.013 | 0.259 | 0.005 | 0.201 | 0.020 | 0.21 | 50.9 | - | 52 | - | 3273 | 22 | 3253 | 18 | 3241 | 31 | 100 | | | |
| 1.1 | 24.378 | 0.435 | 0.662 | 0.006 | 1.511 | 0.013 | 0.267 | 0.005 | 0.159 | 0.005 | 0.15 | 66.3 | 13.8 | 68 | 0.20 | 3274 | 22 | 3284 | 17 | 3290 | 29 | 99 | | | |
| 3.1 | 24.879 | 0.420 | 0.668 | 0.005 | 1.497 | 0.012 | 0.270 | 0.005 | 0.190 | 0.010 | 0.18 | 70 | 12.8 | 72.9 | 0.18 | 3298 | 20 | 3304 | 17 | 3307 | 28 | 99 | | | |
| 36.1 | 23.481 | 0.543 | 0.669 | 0.007 | 1.496 | 0.015 | 0.255 | 0.006 | 0.135 | 0.014 | 0.16 | 29.1 | 19.2 | 30.7 | 0.63 | 3300 | 25 | 3247 | 24 | 3215 | 40 | 102 | | | |
| 6.1 | 25.327 | 0.479 | 0.676 | 0.007 | 1.479 | 0.014 | 0.272 | 0.006 | 0.134 | 0.006 | 0.17 | 44.6 | 13.3 | 45.3 | 0.29 | 3329 | 25 | 3321 | 19 | 3316 | 32 | 100 | Concordia Age: 3339 \pm 7.2 | | |
| 13.1 | 25.486 | 0.475 | 0.682 | 0.006 | 1.466 | 0.012 | 0.271 | 0.005 | 0.176 | 0.012 | 0.32 | 81.2 | 30.8 | 82.7 | 0.37 | 3353 | 21 | 3327 | 18 | 3312 | 28 | 101 | | | |
| 15.1 | 25.823 | 0.491 | 0.685 | 0.006 | 1.460 | 0.012 | 0.274 | 0.005 | 0.153 | 0.010 | 0.16 | 46.3 | 0.4 | 47.8 | 0.01 | 3363 | 22 | 3340 | 19 | 3326 | 30 | 101 | | | |
| 24.1 | 25.285 | 0.494 | 0.685 | 0.006 | 1.459 | 0.013 | 0.268 | 0.005 | 0.208 | 0.012 | 0.31 | 16.9 | 23.5 | 16.8 | 1.40 | 3365 | 24 | 3309 | 19 | 3292 | 31 | 102 | | | |
| 4.1 | 25.635 | 0.427 | 0.687 | 0.005 | 1.456 | 0.011 | 0.271 | 0.005 | 0.248 | 0.019 | 0.09 | 78.5 | 59.8 | 77.1 | 0.78 | 3370 | 20 | 3333 | 16 | 3310 | 27 | 101 | | | |
| 19.1 | 21.398 | 0.562 | 0.604 | 0.009 | 1.656 | 0.024 | 0.257 | 0.007 | 0.243 | 0.042 | 1.42 | 3.9 | - | 4.3 | - | 3045 | 35 | 3157 | 26 | 3229 | 46 | 94 | | | |
| 38.1 | 20.805 | 0.712 | 0.605 | 0.011 | 1.654 | 0.029 | 0.250 | 0.009 | 0.218 | 0.030 | 0.95 | 5.6 | - | 6.2 | - | 3048 | 42 | 3130 | 33 | 3182 | 59 | 95 | | | |
| 21.1 | 21.523 | 0.418 | 0.609 | 0.006 | 1.642 | 0.015 | 0.256 | 0.005 | 0.121 | 0.015 | 1.77 | 7.7 | - | 8.8 | - | 3067 | 23 | 3162 | 20 | 3224 | 32 | 95 | | | |
| 42.1 | 20.377 | 0.735 | 0.617 | 0.012 | 1.621 | 0.031 | 0.240 | 0.009 | 0.213 | 0.065 | 1.00 | 5.8 | 36.6 | 7.3 | 5.05 | 3098 | 47 | 3109 | 36 | 3117 | 64 | 99 | | | |
| 5.1 | 21.543 | 0.390 | 0.619 | 0.005 | 1.616 | 0.013 | 0.253 | 0.005 | 0.115 | 0.047 | 1.48 | 15 | - | 22 | - | 3105 | 20 | 3163 | 17 | 3200 | 29 | 97 | | | |
| 29.1 | 20.898 | 0.483 | 0.626 | 0.011 | 1.598 | 0.028 | 0.242 | 0.007 | 0.192 | 0.032 | 1.02 | 4.2 | 9.1 | 5.7 | 1.59 | 3134 | 45 | 3134 | 27 | 3134 | 48 | 99 | | | |
| 23.1 | 21.775 | 0.665 | 0.633 | 0.012 | 1.581 | 0.029 | 0.250 | 0.009 | 0.218 | 0.023 | 0.56 | 18.6 | 6.5 | 23.4 | 0.28 | 3160 | 47 | 3174 | 32 | 3183 | 56 | 99 | | | |
| 32.1 | 22.866 | 0.499 | 0.634 | 0.005 | 1.578 | 0.013 | 0.262 | 0.006 | 0.165 | 0.006 | 0.24 | 49.9 | 22.2 | 54 | 0.41 | 3165 | 21 | 3221 | 21 | 3257 | 33 | 97 | | | |
| 28.1 | 23.388 | 0.354 | 0.635 | 0.007 | 1.574 | 0.017 | 0.267 | 0.004 | 0.188 | 0.016 | 0.04 | 42.9 | 26.7 | 46.3 | 0.58 | 3170 | 27 | 3243 | 14 | 3289 | 24 | 96 | | | |
| 8.1 | 23.228 | 0.409 | 0.637 | 0.005 | 1.571 | 0.013 | 0.265 | 0.005 | 0.153 | 0.020 | 0.04 | 53.3 | 13 | 60.4 | 1.22 | 3176 | 21 | 3237 | 17 | 3275 | 29 | 96 | | | |
| 3.1 | 21.434 | 0.670 | 0.638 | 0.009 | 1.568 | 0.023 | 0.244 | 0.008 | 0.210 | 0.014 | 0.79 | 8.4 | 9.8 | 9.5 | 1.03 | 3180 | 35 | 3158 | 29 | 3145 | 48 | 101 | | | |
| 22.1 | 22.664 | 0.570 | 0.638 | 0.009 | 1.568 | 0.021 | 0.258 | 0.007 | 0.227 | 0.020 | 0.38 | 18.8 | 10.9 | 27.1 | 0.40 | 3180 | 33 | 3213 | 25 | 3233 | 43 | 98 | | | |
| 18.1 | 23.646 | 0.456 | 0.643 | 0.005 | 1.555 | 0.012 | 0.267 | 0.005 | 0.193 | 0.022 | 0.20 | 30.9 | 4 | 34.8 | 1.12 | 3201 | 19 | 3254 | 18 | 3287 | 29 | 97 | | | |
| 17.1 | 23.531 | 0.448 | 0.646 | 0.005 | 1.547 | 0.013 | 0.264 | 0.005 | 0.174 | 0.008 | 0.17 | 62 | 11.6 | 65.2 | 0.18 | 3214 | 20 | 3249 | 18 | 3271 | 28 | 98 | | | |
| 31.1 | 21.866 | 0.428 | 0.607 | 0.004 | 1.648 | 0.012 | 0.261 | 0.005 | 0.168 | 0.051 | 0.14 | 65 | 13.2 | 114 | 0.12 | 3058 | 18 | 3178 | 20 | 3254 | 32 | 93 | | | |
| 16.1 | 22.507 | 0.419 | 0.609 | 0.005 | 1.642 | 0.013 | 0.268 | 0.005 | 0.196 | 0.029 | 0.11 | 12.3 | 22.5 | 6.8 | 3.31 | 3066 | 19 | 3206 | 18 | 3295 | 28 | 93 | | | |
| 39.1 | 24.905 | 0.526 | 0.671 | 0.005 | 1.491 | 0.012 | 0.269 | 0.006 | 0.172 | 0.008 | 0.14 | 60.1 | 61.8 | 62.5 | 0.99 | 3308 | 21 | 3305 | 20 | 3302 | 32 | 100 | | | |
| 11.1 | 24.770 | 0.454 | 0.673 | 0.006 | 1.487 | 0.013 | 0.267 | 0.005 | 0.140 | 0.012 | 0.25 | 57.5 | 51.3 | 67.5 | 0.76 | 3316 | 23 | 3299 | 18 | 3289 | 30 | 100 | | | |
| 14.1 | 11.122 | 0.253 | 0.349 | 0.003 | 2.865 | 0.027 | 0.231 | 0.005 | 0.127 | 0.018 | 0.16 | 43.2 | 8.1 | 87.9 | 0.09 | 1930 | 15 | 2533 | 18 | 3060 | 31 | 63 | | | |
| 9.1 | 13.730 | 0.306 | 0.481 | 0.005 | 2.081 | 0.022 | 0.207 | 0.005 | 0.047 | 0.008 | 0.34 | 27.9 | 17.5 | 48.6 | 0.36 | 2529 | 23 | 2731 | 22 | 2884 | 42 | 87 | | | |
| 40.1 | 16.781 | 0.543 | 0.521 | 0.007 | 1.920 | 0.026 | 0.234 | 0.007 | 0.196 | 0.020 | 0.28 | 21.1 | 17.1 | 30.2 | 0.57 | 2703 | 29 | 2922 | 27 | 3077 | 47 | 87 | | | |
| 7.1 | 15.181 | 0.628 | 0.543 | 0.013 | 1.843 | 0.045 | 0.203 | 0.010 | 0.058 | 0.036 | 2.80 | 2.1 | 2.1 | 3.8 | 0.56 | 2795 | 55 | 2827 | 41 | 2850 | 84 | 98 | | | |

(continued on next page)

Table I (continued)

| # | RATIOS | | | | | | | | | | | | AGES | | | | | | Conc.206/238 vs 207/206 | Interpretation (Ma) | | |
|---|----------------|------------|----------------|------------|----------------|------------|-----------------|------------|-----------------|------------|---------|------------|-----------|----------|-------------|--------------|------------|--------------|----------------------------|------------------------|------------|--------------|
| | 207Pb/ 235U | 1 σ | 206Pb/ 238U | 1 σ | 238U/ 206Pb | 1 σ | 207Pb/ 206Pb | 1 σ | 208Pb/ 206Pb | 1 σ | Pb* (%) | Pb* ppm | Th ppm | U ppm | Th/U | T206/ 238 | 1 σ | T207/ 235 | | | 1 σ | T207/ 206 |
| CNP13F - Layered amphibole - bearing orthogneiss | | | | | | | | | | | | | | | | | | | | | | |
| 20.1 | 18.475 | 0.385 | 0.547 | 0.005 | 1.829 | 0.018 | 0.245 | 0.005 | 0.134 | 0.011 | 0.21 | 49.1 | 25.4 | 65.5 | 0.39 | 2812 | 22 | 3015 | 20 | 3153 | 34 | 89 |
| 37.1 | 26.053 | 0.550 | 0.701 | 0.006 | 1.426 | 0.012 | 0.270 | 0.006 | 0.220 | 0.019 | 0.32 | 21.5 | - | 22.8 | - | 3425 | 22 | 3349 | 21 | 3303 | 33 | 103 |
| 10.1 | 26.264 | 0.487 | 0.702 | 0.007 | 1.424 | 0.013 | 0.271 | 0.005 | 0.139 | 0.013 | 0.24 | 65.3 | 58.6 | 65.8 | 0.89 | 3429 | 25 | 3356 | 18 | 3314 | 33 | 103 |
| CNP77 - Augen Gneiss (muscovite-bearing mylonitic orthogneiss) | | | | | | | | | | | | | | | | | | | | | | |
| 21.1 | 20.296 | 0.691 | 0.608 | 0.011 | 1.646 | 0.029 | 0.242 | 0.009 | 0.018 | 0.017 | 1.22 | 15 | 19.5 | 20 | 0.98 | 3060 | 43 | 3106 | 32 | 3135 | 61 | 97 |
| Concordia Age: 3078 ± 30 | | | | | | | | | | | | | | | | | | | | | | |
| 24.1 | 18.297 | 0.467 | 0.610 | 0.007 | 1.639 | 0.019 | 0.218 | 0.006 | 0.056 | 0.024 | 2.19 | 12.9 | - | 17.9 | - | 3071 | 28 | 3006 | 26 | 2962 | 48 | 103 |
| 1.1 | 19.519 | 0.406 | 0.613 | 0.006 | 1.630 | 0.015 | 0.231 | 0.005 | 0.018 | 0.006 | 0.46 | 39 | 56.1 | 53 | 1.06 | 3084 | 22 | 3068 | 20 | 3058 | 32 | 100 |
| 6.1 | 18.933 | 0.644 | 0.615 | 0.012 | 1.625 | 0.031 | 0.223 | 0.008 | 0.151 | 0.063 | 0.37 | 20.7 | 28.2 | 25.7 | 1.10 | 3091 | 48 | 3038 | 33 | 3004 | 60 | 102 |
| 27.1 | 20.255 | 0.380 | 0.623 | 0.005 | 1.605 | 0.012 | 0.236 | 0.004 | 0.006 | 0.005 | 3.70 | 55.3 | 23.2 | 75.1 | 0.31 | 3122 | 18 | 3104 | 18 | 3092 | 29 | 100 |
| 16.1 | 24.435 | 0.503 | 0.667 | 0.006 | 1.500 | 0.012 | 0.266 | 0.006 | 0.201 | 0.019 | 0.05 | 43.1 | - | 44.1 | - | 3293 | 21 | 3286 | 20 | 3282 | 33 | 100 |
| 10.1 | 23.869 | 0.608 | 0.675 | 0.009 | 1.482 | 0.021 | 0.257 | 0.007 | 0.286 | 0.023 | 0.57 | 14.5 | - | 13.9 | - | 3324 | 36 | 3263 | 25 | 3226 | 42 | 103 |
| 20.1 | 25.306 | 0.516 | 0.675 | 0.005 | 1.482 | 0.012 | 0.272 | 0.006 | 0.235 | 0.014 | 0.00 | 73.7 | 23.1 | 75.4 | 0.31 | 3324 | 20 | 3320 | 20 | 3318 | 32 | 100 |
| 3.1 | 24.398 | 0.516 | 0.675 | 0.006 | 1.481 | 0.014 | 0.262 | 0.006 | 0.108 | 0.045 | 0.10 | 64.8 | 58.7 | 68.6 | 0.86 | 3326 | 25 | 3284 | 20 | 3259 | 33 | 102 |
| 21.1 | 17.125 | 0.522 | 0.591 | 0.008 | 1.692 | 0.024 | 0.210 | 0.007 | 0.087 | 0.018 | 0.79 | 7.6 | 30 | 11 | 2.73 | 2993 | 33 | 2942 | 29 | 2907 | 56 | 102 |
| 9.1 | 17.392 | 0.807 | 0.592 | 0.018 | 1.689 | 0.050 | 0.213 | 0.012 | 0.065 | 0.044 | 0.50 | 3.4 | - | 6.1 | - | 2997 | 72 | 2957 | 47 | 2929 | 91 | 102 |
| 26.1 | 17.275 | 0.286 | 0.576 | 0.004 | 1.736 | 0.011 | 0.218 | 0.004 | 0.067 | 0.011 | 0.05 | 53.3 | 30.8 | 65.8 | 0.47 | 2932 | 14 | 2950 | 17 | 2963 | 27 | 98 |
| 29.1 | 18.365 | 0.340 | 0.598 | 0.004 | 1.672 | 0.012 | 0.223 | 0.004 | 0.017 | 0.008 | 0.00 | 27.8 | 48 | 38.7 | 1.24 | 3022 | 17 | 3009 | 18 | 3001 | 29 | 100 |
| 14.1 | 15.83 | 0.113 | 0.167 | 0.003 | 5.994 | 0.097 | 0.069 | 0.006 | 0.310 | 0.017 | 1.69 | 11.5 | 21.1 | 49.5 | 0.43 | 995 | 15 | 964 | 44 | 894 | 160 | 111 |
| 11.1 | 4.979 | 0.149 | 0.323 | 0.004 | 3.100 | 0.035 | 0.112 | 0.004 | 0.291 | 0.012 | 0.85 | 42.1 | 61.3 | 96.8 | 0.63 | 1803 | 18 | 1816 | 25 | 1831 | 59 | 98 |
| 15.1 | 10.794 | 0.412 | 0.479 | 0.007 | 2.088 | 0.031 | 0.164 | 0.007 | 0.047 | 0.025 | 0.98 | 7.7 | 30.7 | 18 | 1.71 | 2523 | 30 | 2506 | 29 | 2492 | 56 | 101 |
| 7.1 | 13.478 | 0.566 | 0.533 | 0.012 | 1.875 | 0.043 | 0.183 | 0.009 | 0.067 | 0.029 | 0.57 | 13.8 | 6.3 | 25.1 | 0.25 | 2756 | 50 | 2714 | 37 | 2683 | 72 | 102 |
| 28.2 | 14.761 | 0.333 | 0.572 | 0.005 | 1.747 | 0.016 | 0.187 | 0.004 | 0.023 | 0.007 | 0.30 | 28.3 | 39.8 | 39.5 | 1.01 | 2917 | 22 | 2800 | 21 | 2717 | 38 | 107 |
| 22.1 | 15.698 | 0.745 | 0.565 | 0.014 | 1.769 | 0.043 | 0.201 | 0.012 | 0.065 | 0.025 | 3.48 | 2.2 | - | 4.5 | - | 2889 | 58 | 2859 | 47 | 2837 | 99 | 101 |
| 18.1 | 16.612 | 0.704 | 0.590 | 0.012 | 1.696 | 0.035 | 0.204 | 0.010 | 0.180 | 0.041 | 5.49 | 1.4 | - | 2.2 | - | 2987 | 49 | 2913 | 38 | 2862 | 78 | 104 |
| Concordia Age: 3298±9 | | | | | | | | | | | | | | | | | | | | | | |
| 33.1 | 16.115 | 0.340 | 0.569 | 0.004 | 1.757 | 0.013 | 0.205 | 0.004 | 0.016 | 0.021 | 0.17 | 27.3 | 31.1 | 36 | 0.86 | 2905 | 17 | 2884 | 18 | 2869 | 29 | 101 |
| 14.1 | 16.562 | 0.354 | 0.559 | 0.005 | 1.789 | 0.014 | 0.215 | 0.005 | 0.024 | 0.007 | 4.13 | 60.1 | 9.2 | 86.9 | 0.11 | 2862 | 19 | 2910 | 20 | 2943 | 35 | 97 |
| 31.1 | 17.062 | 0.327 | 0.564 | 0.004 | 1.774 | 0.013 | 0.220 | 0.004 | 0.018 | 0.005 | 0.57 | 57.1 | - | 79.3 | - | 2882 | 17 | 2938 | 18 | 2977 | 31 | 96 |
| 35.1 | 20.508 | 0.410 | 0.638 | 0.005 | 1.568 | 0.013 | 0.233 | 0.005 | 0.011 | 0.016 | 0.43 | 21.2 | 40.3 | 27 | 1.49 | 3181 | 20 | 3116 | 19 | 3074 | 31 | 103 |
| Concordia Age: 2965±41 | | | | | | | | | | | | | | | | | | | | | | |
| 28.1 | 20.642 | 0.388 | 0.627 | 0.005 | 1.594 | 0.012 | 0.239 | 0.004 | 0.002 | 0.002 | 0.34 | 72.4 | 0.3 | 94.4 | 0.00 | 3140 | 18 | 3122 | 18 | 3111 | 28 | 100 |
| 13.1 | 21.695 | 0.475 | 0.635 | 0.006 | 1.575 | 0.015 | 0.248 | 0.006 | 0.010 | 0.006 | 0.44 | 38.7 | 50.4 | 49.2 | 1.03 | 3170 | 24 | 3170 | 22 | 3170 | 38 | 99 |
| 2.1 | 23.527 | 0.500 | 0.681 | 0.007 | 1.468 | 0.015 | 0.251 | 0.005 | 0.007 | 0.006 | 1.05 | 80 | 40.2 | 94.8 | 0.43 | 3349 | 26 | 3249 | 21 | 3188 | 34 | 105 |
| 17.1 | 23.419 | 0.489 | 0.662 | 0.006 | 1.511 | 0.013 | 0.257 | 0.006 | 0.015 | 0.003 | 0.14 | 61.5 | 42 | 72.8 | 0.58 | 3275 | 21 | 3245 | 20 | 3226 | 34 | 101 |
| 12.1 | 22.482 | 0.475 | 0.635 | 0.006 | 1.575 | 0.015 | 0.257 | 0.006 | 0.145 | 0.010 | 0.00 | 54.2 | 24.1 | 61.3 | 0.39 | 3168 | 24 | 3205 | 21 | 3228 | 34 | 98 |
| 25.1 | 21.863 | 0.482 | 0.617 | 0.006 | 1.620 | 0.017 | 0.257 | 0.006 | 0.098 | 0.024 | 0.49 | 41.2 | 31.3 | 52.2 | 0.60 | 3099 | 25 | 3178 | 21 | 3228 | 35 | 95 |
| 40.1 | 25.983 | 0.524 | 0.715 | 0.006 | 1.399 | 0.012 | 0.264 | 0.005 | 0.246 | 0.038 | 0.28 | 22.9 | 28.3 | 24.8 | 1.14 | 3476 | 22 | 3346 | 19 | 3269 | 30 | 106 |
| 3.1 | 23.653 | 0.504 | 0.645 | 0.007 | 1.590 | 0.016 | 0.266 | 0.006 | 0.167 | 0.006 | 0.37 | 7.6 | 9.9 | 81.7 | 0.12 | 3210 | 25 | 3254 | 21 | 3282 | 34 | 97 |
| 32.1 | 23.190 | 0.458 | 0.621 | 0.005 | 1.611 | 0.013 | 0.271 | 0.005 | 0.162 | 0.016 | 0.53 | 58.5 | 11.9 | 61.9 | 0.19 | 3113 | 21 | 3235 | 19 | 3312 | 30 | 93 |
| MiZ1 - Amphibole - bearing orthogneiss | | | | | | | | | | | | | | | | | | | | | | |
| 31.1 | 10.832 | 0.194 | 0.443 | 0.004 | 2.257 | 0.023 | 0.177 | 0.003 | 0.021 | 0.009 | 0.24 | 105.7 | 16.9 | 295 | 0.06 | 2365 | 0.02 | 2509 | 0.02 | 2628 | 0 | 89 |
| 18.1 | 15.832 | 0.239 | 0.550 | 0.006 | 1.817 | 0.018 | 0.209 | 0.003 | 0.062 | 0.008 | 0.12 | 187.5 | 80.9 | 308 | 0.26 | 2826 | 0.02 | 2867 | 0.02 | 2895 | 0 | 97 |
| 13.1 | 17.318 | 0.310 | 0.571 | 0.006 | 1.752 | 0.017 | 0.220 | 0.004 | 0.149 | 0.066 | 0.16 | 187.4 | 319 | 216 | 1.48 | 2911 | 0.02 | 2953 | 0.02 | 2981 | 0 | 97 |
| 17.1 | 17.222 | 0.188 | 0.574 | 0.005 | 1.742 | 0.014 | 0.218 | 0.003 | 0.104 | 0.069 | 0.00 | 251 | 385 | 234 | 1.64 | 2925 | 0.02 | 2947 | 0.01 | 2962 | 0 | 98 |

(continued on next page)

Table I (continued)

| # | RATIOS | | | | | | | | | Pb* (%) | Pb* ppm | Th ppm | U ppm | Th/U | AGES | | | | | | Conc.206/238 vs 207/206 | Interpretation (Ma) | |
|--|-------------|------------|-------------|------------|-------------|------------|--------------|------------|--------------|---------|---------|--------|-------|------|-------------|-----------|------------|-----------|------------|-----------|-------------------------|---------------------|--------------------------------|
| | 207Pb/ 235U | 1 σ | 206Pb/ 238U | 1 σ | 238U/ 206Pb | 1 σ | 207Pb/ 206Pb | 1 σ | 208Pb/ 206Pb | | | | | | 1 σ | T206/ 238 | 1 σ | T207/ 235 | 1 σ | T207/ 206 | | | 1 σ |
| CNP13F - Layered amphibole - bearing orthogneiss | | | | | | | | | | | | | | | | | | | | | | | |
| 21.1 | 17.472 | 0.336 | 0.580 | 0.005 | 1.723 | 0.015 | 0.218 | 0.003 | 0.077 | 0.032 | 0.59 | 99.1 | 158 | 124 | 1.27 | 2951 | 0.02 | 2961 | 0.02 | 2968 | 0 | 99 | |
| 36.1 | 17.662 | 0.269 | 0.584 | 0.007 | 1.711 | 0.021 | 0.219 | 0.003 | 0.153 | 0.107 | 0.00 | 60.4 | 48.8 | 98.8 | 0.49 | 2966 | 0.03 | 2972 | 0.02 | 2975 | 0 | 99 | |
| 33.1 | 17.819 | 0.331 | 0.587 | 0.008 | 1.703 | 0.024 | 0.220 | 0.003 | 0.273 | 0.006 | 0.35 | 43.7 | 54.9 | 56.7 | 0.97 | 2979 | 0.03 | 2980 | 0.02 | 2981 | 0 | 99 | |
| 9.1 | 19.156 | 0.365 | 0.608 | 0.007 | 1.644 | 0.019 | 0.228 | 0.004 | 0.169 | 0.094 | 0.02 | 95 | 56.2 | 119 | 0.47 | 3063 | 0.03 | 3050 | 0.02 | 3041 | 0 | 100 | |
| 23.1 | 18.772 | 0.358 | 0.612 | 0.005 | 1.634 | 0.014 | 0.223 | 0.003 | 0.132 | 0.062 | 0.47 | 280.6 | 515 | 281 | 1.83 | 3077 | 0.02 | 3030 | 0.02 | 2999 | 0 | 102 | Li: 1804 \pm 17 |
| 15.1 | 19.094 | 0.282 | 0.612 | 0.006 | 1.633 | 0.016 | 0.226 | 0.003 | 0.104 | 0.038 | 0.00 | 66.3 | 49.3 | 79.9 | 0.62 | 3080 | 0.02 | 3047 | 0.02 | 3025 | 0 | 101 | |
| 1.1 | 19.973 | 0.514 | 0.616 | 0.010 | 1.624 | 0.025 | 0.235 | 0.004 | 0.178 | 0.004 | 0.04 | 73.7 | 67 | 92.8 | 0.72 | 3094 | 0.04 | 3090 | 0.02 | 3088 | 0 | 100 | |
| 5.1 | 19.645 | 0.476 | 0.617 | 0.009 | 1.622 | 0.024 | 0.231 | 0.003 | 0.178 | 0.004 | 0.01 | 76.6 | 85 | 119 | 0.72 | 3096 | 0.04 | 3074 | 0.02 | 3060 | 0 | 101 | |
| 19.1 | 19.308 | 0.277 | 0.621 | 0.006 | 1.612 | 0.016 | 0.226 | 0.003 | 0.137 | 0.065 | 0.04 | 157.3 | 58.3 | 201 | 0.29 | 3112 | 0.02 | 3057 | 0.02 | 3022 | 0 | 102 | |
| 10.1 | 20.085 | 0.420 | 0.622 | 0.008 | 1.607 | 0.021 | 0.234 | 0.005 | 0.225 | 0.009 | 0.00 | 50.9 | 53.1 | 62.3 | 0.85 | 3118 | 0.03 | 3095 | 0.02 | 3081 | 0 | 101 | |
| 7.1 | 20.622 | 0.575 | 0.632 | 0.011 | 1.582 | 0.027 | 0.237 | 0.004 | 0.133 | 0.020 | 0.04 | 68.8 | 69.2 | 86.6 | 0.80 | 3159 | 0.04 | 3121 | 0.03 | 3097 | 0 | 101 | |
| 4.1 | 20.251 | 0.499 | 0.639 | 0.009 | 1.566 | 0.023 | 0.230 | 0.003 | 0.191 | 0.005 | 0.10 | 109.4 | 127 | 147 | 0.86 | 3184 | 0.04 | 3103 | 0.02 | 3052 | 0 | 104 | |
| Mi30 - Migmatite of Route 8 (quartz-feldspathic biotite gneiss with Kfs ad-situ veins) | | | | | | | | | | | | | | | | | | | | | | | |
| 18.1 | 7.722 | 0.175 | 0.382 | 0.006 | 2.621 | 0.038 | 0.147 | 0.003 | 0.019 | 0.007 | 0.00 | 79 | 17 | 124 | 0.14 | 2083 | 0.03 | 2199 | 0.02 | 2309 | 0.03 | 90 | Concordia age: 3074 \pm 7 |
| 16.1 | 16.386 | 0.298 | 0.550 | 0.007 | 1.817 | 0.024 | 0.216 | 0.004 | 0.038 | 0.001 | 0.30 | 160 | 45 | 255 | 0.18 | 2827 | 0.03 | 2900 | 0.02 | 2951 | 0.03 | 95 | |
| 10.1 | 16.718 | 0.349 | 0.559 | 0.009 | 1.790 | 0.028 | 0.217 | 0.003 | 0.087 | 0.008 | 0.12 | 57 | 14 | 85 | 0.16 | 2861 | 0.04 | 2919 | 0.02 | 2959 | 0.02 | 96 | |
| 21.1 | 16.333 | 0.273 | 0.562 | 0.008 | 1.781 | 0.025 | 0.211 | 0.003 | 0.012 | 0.004 | 0.00 | 170 | 13 | 236 | 0.05 | 2873 | 0.03 | 2896 | 0.02 | 2913 | 0.02 | 98 | |
| 32.1 | 17.012 | 0.364 | 0.568 | 0.009 | 1.762 | 0.027 | 0.217 | 0.003 | 0.090 | 0.002 | 0.02 | 103 | 60 | 157 | 0.38 | 2898 | 0.04 | 2935 | 0.02 | 2962 | 0.03 | 97 | |
| 19.1 | 17.513 | 0.320 | 0.577 | 0.008 | 1.732 | 0.023 | 0.220 | 0.004 | 0.021 | 0.003 | 0.05 | 95 | 12 | 145 | 0.08 | 2938 | 0.03 | 2963 | 0.02 | 2981 | 0.03 | 98 | |
| 26.1 | 17.417 | 0.317 | 0.578 | 0.008 | 1.731 | 0.025 | 0.219 | 0.003 | 0.096 | 0.006 | 0.00 | 219 | 108 | 306 | 0.35 | 2939 | 0.03 | 2958 | 0.02 | 2971 | 0.02 | 98 | |
| 11.1 | 17.923 | 0.387 | 0.585 | 0.009 | 1.709 | 0.026 | 0.222 | 0.003 | 0.171 | 0.010 | 1.08 | 140 | 135 | 155 | 0.88 | 2969 | 0.04 | 2986 | 0.02 | 2997 | 0.02 | 99 | |
| 9.1 | 18.075 | 0.368 | 0.597 | 0.009 | 1.674 | 0.024 | 0.219 | 0.003 | 0.155 | 0.025 | 2.37 | 116 | 92 | 168 | 0.55 | 3019 | 0.04 | 2994 | 0.02 | 2977 | 0.02 | 101 | |
| 15.1 | 18.483 | 0.344 | 0.601 | 0.008 | 1.665 | 0.022 | 0.223 | 0.004 | 0.192 | 0.002 | 0.00 | 268 | 294 | 299 | 0.98 | 3032 | 0.03 | 3015 | 0.02 | 3004 | 0.03 | 100 | |
| 17.1 | 18.912 | 0.347 | 0.601 | 0.008 | 1.665 | 0.022 | 0.228 | 0.004 | 0.159 | 0.007 | 0.01 | 109 | 92 | 147 | 0.63 | 3033 | 0.03 | 3037 | 0.02 | 3040 | 0.03 | 99 | |
| 36.1 | 19.144 | 0.348 | 0.603 | 0.009 | 1.659 | 0.026 | 0.230 | 0.003 | 0.097 | 0.007 | 0.00 | 147 | 92 | 186 | 0.50 | 3041 | 0.04 | 3049 | 0.02 | 3055 | 0.02 | 99 | |
| 25.1 | 18.181 | 0.320 | 0.604 | 0.009 | 1.657 | 0.024 | 0.219 | 0.003 | 0.108 | 0.031 | 0.02 | 165 | 98 | 226 | 0.43 | 3044 | 0.04 | 2999 | 0.02 | 2970 | 0.02 | 102 | |
| 13.1 | 18.530 | 0.363 | 0.605 | 0.009 | 1.653 | 0.024 | 0.222 | 0.003 | 0.097 | 0.008 | 1.74 | 242 | 119 | 266 | 0.45 | 3050 | 0.04 | 3018 | 0.02 | 2996 | 0.02 | 101 | |
| 33.1 | 19.208 | 0.412 | 0.605 | 0.009 | 1.652 | 0.026 | 0.230 | 0.004 | 0.121 | 0.010 | 0.19 | 118 | 83 | 155 | 0.54 | 3051 | 0.04 | 3052 | 0.02 | 3053 | 0.03 | 99 | |
| 27.1 | 19.203 | 0.370 | 0.608 | 0.010 | 1.645 | 0.026 | 0.229 | 0.003 | 0.112 | 0.008 | 0.00 | 143 | 107 | 182 | 0.59 | 3062 | 0.04 | 3052 | 0.02 | 3046 | 0.02 | 100 | |
| 5.1 | 19.306 | 0.290 | 0.609 | 0.007 | 1.641 | 0.020 | 0.230 | 0.004 | 0.094 | 0.009 | 0.22 | 99 | 40 | 135 | 0.30 | 3067 | 0.03 | 3057 | 0.01 | 3051 | 0.02 | 100 | |
| 2.2 | 18.960 | 0.285 | 0.610 | 0.008 | 1.640 | 0.020 | 0.226 | 0.003 | 0.093 | 0.001 | 0.19 | 167 | 104 | 231 | 0.45 | 3068 | 0.03 | 3040 | 0.01 | 3021 | 0.02 | 101 | |
| 19.1 | 19.170 | 0.361 | 0.610 | 0.010 | 1.640 | 0.027 | 0.228 | 0.003 | 0.113 | 0.005 | 0.25 | 88 | 39 | 124 | 0.31 | 3069 | 0.04 | 3050 | 0.02 | 3038 | 0.02 | 101 | |
| 30.1 | 18.412 | 0.388 | 0.610 | 0.009 | 1.639 | 0.025 | 0.219 | 0.003 | 0.067 | 0.024 | 0.05 | 216 | 123 | 309 | 0.40 | 3071 | 0.04 | 3011 | 0.02 | 2972 | 0.02 | 103 | Concordia age: 1840 \pm 2 |
| 14.1 | 18.511 | 0.374 | 0.611 | 0.009 | 1.638 | 0.025 | 0.220 | 0.003 | 0.073 | 0.010 | 0.00 | 113 | 44 | 166 | 0.27 | 3072 | 0.04 | 3017 | 0.02 | 2980 | 0.03 | 103 | |
| 22.1 | 18.352 | 0.345 | 0.614 | 0.009 | 1.630 | 0.024 | 0.217 | 0.003 | 0.180 | 0.003 | 0.00 | 14 | 31 | 45 | 0.68 | 3084 | 0.04 | 3008 | 0.02 | 2958 | 0.02 | 104 | |
| 2.1 | 18.706 | 0.291 | 0.618 | 0.008 | 1.619 | 0.020 | 0.220 | 0.003 | 0.166 | 0.003 | 0.00 | 216 | 203 | 229 | 0.89 | 3100 | 0.03 | 3027 | 0.02 | 2978 | 0.02 | 104 | |

(continued on next page)

Table I (continued)

| # | RATIOS | | | | | | | | | | Pb* (%) | Pb* ppm | Th ppm | U ppm | Th/U | AGES | | | | | Conc.206/238 vs 207/206 | Interpretation (Ma) | |
|--|-------------|------------|-------------|------------|-------------|------------|--------------|------------|--------------|------------|---------|---------|--------|-------|-------------|-----------|------------|-----------|------------|-----------|-------------------------|---------------------|--------------------------|
| | 207Pb/ 235U | 1 σ | 206Pb/ 238U | 1 σ | 238U/ 206Pb | 1 σ | 207Pb/ 206Pb | 1 σ | 208Pb/ 206Pb | 1 σ | | | | | | T206/ 238 | 1 σ | T207/ 235 | 1 σ | T207/ 206 | | | 1 σ |
| CNP13F - Layered amphibole - bearing orthogneiss | | | | | | | | | | | | | | | | | | | | | | | |
| 4.1 | 19.438 | 0.290 | 0.618 | 0.008 | 1.619 | 0.020 | 0.228 | 0.004 | 0.117 | 0.002 | 0.00 | 140 | 94 | 180 | 0.52 | 3101 | 0.03 | 3064 | 0.01 | 3040 | 0.02 | 101 | |
| 34.1 | 19.431 | 0.409 | 0.619 | 0.009 | 1.615 | 0.024 | 0.228 | 0.004 | 0.133 | 0.002 | 0.10 | 150 | 128 | 183 | 0.70 | 3107 | 0.04 | 3063 | 0.02 | 3035 | 0.02 | 102 | |
| 6.1 | 18.755 | 0.282 | 0.621 | 0.008 | 1.611 | 0.020 | 0.219 | 0.003 | 0.071 | 0.001 | 0.06 | 127 | 55 | 159 | 0.35 | 3113 | 0.03 | 3029 | 0.02 | 2974 | 0.02 | 104 | |
| 35.1 | 19.622 | 0.446 | 0.623 | 0.010 | 1.606 | 0.027 | 0.229 | 0.004 | 0.091 | 0.005 | 0.71 | 78 | 54 | 108 | 0.50 | 3120 | 0.04 | 3073 | 0.02 | 3042 | 0.03 | 102 | |
| 1.1 | 19.463 | 0.294 | 0.627 | 0.008 | 1.596 | 0.020 | 0.225 | 0.004 | 0.127 | 0.005 | 0.05 | 207 | 168 | 250 | 0.67 | 3136 | 0.03 | 3065 | 0.02 | 3019 | 0.03 | 103 | |
| 7.1 | 19.525 | 0.298 | 0.628 | 0.008 | 1.593 | 0.020 | 0.226 | 0.003 | 0.100 | 0.012 | 0.02 | 140 | 93 | 178 | 0.52 | 3140 | 0.03 | 3068 | 0.02 | 3021 | 0.02 | 103 | |
| 8.1 | 19.534 | 0.387 | 0.628 | 0.009 | 1.592 | 0.023 | 0.226 | 0.003 | 0.117 | 0.002 | 0.00 | 130 | 89 | 170 | 0.52 | 3142 | 0.04 | 3069 | 0.02 | 3021 | 0.02 | 103 | |
| 11.1 | 20.030 | 0.401 | 0.631 | 0.010 | 1.585 | 0.024 | 0.230 | 0.004 | 0.098 | 0.003 | 0.18 | 93 | 45 | 124 | 0.36 | 3153 | 0.04 | 3093 | 0.02 | 3054 | 0.03 | 103 | |
| 20.1 | 17.391 | 0.319 | 0.553 | 0.007 | 1.809 | 0.024 | 0.228 | 0.004 | 0.111 | 0.003 | 0.02 | 167 | 79 | 190 | 0.41 | 2837 | 0.03 | 2957 | 0.02 | 3039 | 0.03 | 93 | |
| 12.1 | 17.529 | 0.360 | 0.559 | 0.009 | 1.790 | 0.028 | 0.228 | 0.004 | 0.078 | 0.003 | 0.39 | 82 | 46.4 | 102 | 0.45 | 2862 | 0.04 | 2964 | 0.02 | 3035 | 0.02 | 94 | |
| 3.1 | 5.490 | 0.092 | 0.345 | 0.004 | 2.903 | 0.036 | 0.116 | 0.002 | 0.085 | 0.051 | 0.00 | 353 | 204 | 852 | 0.24 | 1908 | 0.02 | 1899 | 0.02 | 1889 | 0.02 | 100 | LI: 1917±13 LI: 1037±146 |
| 16.1 | 5.581 | 0.104 | 0.348 | 0.005 | 2.878 | 0.037 | 0.117 | 0.002 | 0.067 | 0.001 | 0.14 | 162 | 92 | 425 | 0.22 | 1923 | 0.02 | 1913 | 0.02 | 1903 | 0.03 | 101 | |
| 15.1 | 5.691 | 0.098 | 0.351 | 0.004 | 2.852 | 0.034 | 0.118 | 0.002 | 0.063 | 0.010 | 0.00 | 184 | 92 | 494 | 0.19 | 1937 | 0.02 | 1930 | 0.02 | 1922 | 0.03 | 100 | |
| 35.1 | 5.753 | 0.103 | 0.350 | 0.004 | 2.854 | 0.032 | 0.119 | 0.002 | 0.046 | 0.001 | 0.04 | 235 | 87 | 548 | 0.16 | 1937 | 0.02 | 1939 | 0.02 | 1942 | 0.03 | 99 | |
| 6.1 | 6.030 | 0.108 | 0.361 | 0.005 | 2.774 | 0.036 | 0.121 | 0.002 | 0.098 | 0.004 | 0.00 | 109 | 78 | 268 | 0.29 | 1985 | 0.02 | 1980 | 0.02 | 1976 | 0.03 | 100 | LI: 1986±18 |
| 22.1 | 5.959 | 0.092 | 0.365 | 0.004 | 2.744 | 0.032 | 0.119 | 0.002 | 0.109 | 0.088 | 0.00 | 364 | 174 | 809 | 0.22 | 2003 | 0.02 | 1970 | 0.01 | 1935 | 0.03 | 103 | |
| 7.1 | 6.100 | 0.108 | 0.365 | 0.005 | 2.740 | 0.034 | 0.121 | 0.002 | 0.093 | 0.002 | 0.03 | 144 | 85 | 348 | 0.24 | 2006 | 0.02 | 1990 | 0.02 | 1974 | 0.03 | 101 | |
| 34.1 | 6.115 | 0.110 | 0.367 | 0.004 | 2.728 | 0.031 | 0.121 | 0.002 | 0.087 | 0.006 | 0.00 | 184 | 137 | 438 | 0.31 | 2014 | 0.02 | 1992 | 0.02 | 1971 | 0.03 | 102 | |
| 5.1 | 6.184 | 0.110 | 0.368 | 0.005 | 2.720 | 0.034 | 0.122 | 0.002 | 0.110 | 0.002 | 0.24 | 104 | 69 | 239 | 0.29 | 2018 | 0.02 | 2002 | 0.02 | 1986 | 0.03 | 101 | |
| 24.1 | 6.055 | 0.093 | 0.368 | 0.004 | 2.714 | 0.032 | 0.119 | 0.002 | 0.082 | 0.020 | 0.15 | 182 | 214 | 413 | 0.52 | 2022 | 0.02 | 1984 | 0.01 | 1944 | 0.03 | 104 | |
| 1.1 | 12.929 | 0.221 | 0.485 | 0.006 | 2.064 | 0.026 | 0.194 | 0.003 | 0.031 | 0.002 | 0.25 | 405 | 96 | 725 | 0.13 | 2547 | 0.03 | 2674 | 0.02 | 2772 | 0.02 | 91 | LI: 2973±15 |
| 14.1 | 14.778 | 0.291 | 0.532 | 0.007 | 1.880 | 0.026 | 0.202 | 0.003 | 0.055 | 0.005 | 0.00 | 76 | 38 | 96 | 0.39 | 2750 | 0.03 | 2801 | 0.02 | 2838 | 0.03 | 96 | |
| 4.1 | 16.598 | 0.303 | 0.573 | 0.008 | 1.746 | 0.023 | 0.210 | 0.003 | 0.078 | 0.004 | 0.75 | 169 | 61 | 204 | 0.30 | 2919 | 0.03 | 2912 | 0.02 | 2907 | 0.02 | 100 | |
| 30.1 | 17.422 | 0.323 | 0.593 | 0.007 | 1.686 | 0.021 | 0.213 | 0.004 | 0.056 | 0.002 | 0.00 | 238 | 81 | 305 | 0.27 | 3002 | 0.03 | 2958 | 0.02 | 2929 | 0.03 | 102 | |
| 2.1 | 18.908 | 0.332 | 0.630 | 0.008 | 1.588 | 0.021 | 0.218 | 0.003 | 0.109 | 0.010 | 0.00 | 172 | 116 | 222 | 0.52 | 3149 | 0.03 | 3037 | 0.02 | 2964 | 0.02 | 106 | |
| 29.1 | 17.649 | 0.259 | 0.577 | 0.007 | 1.733 | 0.020 | 0.222 | 0.003 | 0.073 | 0.016 | 0.52 | 88 | 59 | 161 | 0.36 | 2937 | 0.03 | 2971 | 0.01 | 2994 | 0.02 | 98 | |
| 8.1 | 18.409 | 0.339 | 0.597 | 0.008 | 1.675 | 0.023 | 0.224 | 0.003 | 0.124 | 0.029 | 0.03 | 211 | 217 | 241 | 0.90 | 3018 | 0.03 | 3011 | 0.02 | 3007 | 0.02 | 100 | |
| 31.1 | 18.374 | 0.358 | 0.594 | 0.007 | 1.683 | 0.020 | 0.224 | 0.004 | 0.080 | 0.005 | 0.27 | 35 | 13 | 76 | 0.17 | 3007 | 0.03 | 3010 | 0.02 | 3011 | 0.03 | 99 | |
| 26.1 | 19.170 | 0.286 | 0.620 | 0.007 | 1.612 | 0.018 | 0.224 | 0.003 | 0.096 | 0.012 | 0.13 | 199 | 134 | 241 | 0.55 | 3111 | 0.03 | 3050 | 0.01 | 3011 | 0.02 | 103 | |
| 19.1 | 4.876 | 0.088 | 0.313 | 0.004 | 3.194 | 0.040 | 0.113 | 0.002 | 0.039 | 0.008 | 0.58 | 96 | 69 | 176 | 0.39 | 1756 | 0.02 | 1798 | 0.02 | 1847 | 0.03 | 95 | LI: 1887±28 |
| 12.1 | 6.170 | 0.123 | 0.374 | 0.005 | 2.677 | 0.037 | 0.120 | 0.002 | 0.086 | 0.004 | 0.12 | 89 | 59 | 204 | 0.29 | 2046 | 0.02 | 2000 | 0.02 | 1953 | 0.03 | 104 | |
| 28.1 | 6.165 | 0.087 | 0.372 | 0.004 | 2.692 | 0.026 | 0.120 | 0.002 | 0.096 | 0.003 | 1.31 | 103 | 104 | 330 | 0.32 | 2036 | 0.02 | 1999 | 0.01 | 1962 | 0.02 | 103 | |
| 33.1 | 6.526 | 0.123 | 0.390 | 0.005 | 2.563 | 0.030 | 0.121 | 0.002 | 0.063 | 0.001 | 0.00 | 267 | 141 | 624 | 0.23 | 2124 | 0.02 | 2049 | 0.02 | 1975 | 0.03 | 107 | |
| 25.1 | 5.878 | 0.095 | 0.344 | 0.004 | 2.905 | 0.032 | 0.124 | 0.002 | 0.087 | 0.006 | 1.45 | 98 | 80 | 205 | 0.39 | 1907 | 0.02 | 1958 | 0.01 | 2012 | 0.03 | 94 | |
| 23.1 | 9.642 | 0.245 | 0.507 | 0.006 | 1.971 | 0.024 | 0.138 | 0.004 | 0.046 | 0.005 | 0.34 | 473 | 149 | 684 | 0.22 | 2646 | 0.03 | 2401 | 0.02 | 2200 | 0.03 | 120 | |
| 11.1 | 7.400 | 0.142 | 0.385 | 0.005 | 2.596 | 0.034 | 0.139 | 0.002 | 0.048 | 0.005 | 0.10 | 233 | 94 | 379 | 0.25 | 2101 | 0.02 | 2161 | 0.02 | 2218 | 0.03 | 94 | |
| 36.1 | 12.043 | 0.210 | 0.509 | 0.006 | 1.967 | 0.022 | 0.172 | 0.003 | 0.031 | 0.002 | 0.00 | 105 | 20 | 158 | 0.12 | 2650 | 0.02 | 2608 | 0.02 | 2575 | 0.03 | 102 | |
| 17.1 | 13.098 | 0.261 | 0.451 | 0.006 | 2.220 | 0.030 | 0.211 | 0.003 | 0.040 | 0.003 | 0.06 | 206 | 47 | 245 | 0.19 | 2397 | 0.03 | 2687 | 0.02 | 2912 | 0.03 | 82 | |

(continued on next page)

Table I (continued)

| # | 207Pb/235U | | RATIOS | | 208Pb/238U | | 207Pb/206Pb | | 208Pb/206Pb | | Pb* (%) | | CN131E - Layered amphibole - bearing orthopyroxene | | Th ppm | U ppm | Th/U | T206/238 | ACES | | TZ07/206 | 1σ | Conc.206/238 vs 207/206 | Interpretation (Ma) | |
|-----|------------|-------|--------|-------|------------|-------|-------------|-------|-------------|-------|---------|-----|--|-----|-------------|-------|------|----------|------|------|----------|-----|-------------------------|---------------------|--------------|
| | 1σ | 1σ | 1σ | 1σ | 1σ | 1σ | 1σ | 1σ | 1σ | 1σ | 1σ | 1σ | 1σ | 1σ | | | | | 1σ | 1σ | | | | | 1σ |
| 71 | 2.522 | 0.100 | 0.193 | 0.004 | 5.191 | 0.106 | 0.095 | 0.002 | 0.163 | 0.051 | 3.30 | 167 | 699 | 670 | 1.04 | 1136 | 0.01 | 1278 | 0.01 | 1527 | 0.02 | 74 | | | UH: 1987±3.2 |
| 841 | 4.841 | 0.072 | 0.299 | 0.003 | 3.347 | 0.032 | 0.118 | 0.002 | 0.114 | 0.007 | 0.14 | 106 | 205 | 345 | 1.60 | 1655 | 0.01 | 1702 | 0.01 | 1919 | 0.02 | 87 | | | |
| 241 | 5.313 | 0.111 | 0.318 | 0.003 | 3.149 | 0.034 | 0.121 | 0.002 | 0.147 | 0.022 | 0.00 | 102 | 123 | 275 | 0.45 | 1778 | 0.01 | 1871 | 0.01 | 1576 | 0.02 | 89 | | | |
| 181 | 5.393 | 0.068 | 0.329 | 0.003 | 3.040 | 0.023 | 0.119 | 0.002 | 0.152 | 0.033 | 1.88 | 100 | 145 | 262 | 0.55 | 1833 | 0.01 | 1884 | 0.01 | 1940 | 0.02 | 94 | | | |
| 121 | 5.390 | 0.080 | 0.329 | 0.004 | 3.077 | 0.035 | 0.120 | 0.002 | 0.111 | 0.011 | 0.00 | 110 | 98 | 288 | 0.34 | 1835 | 0.01 | 1883 | 0.01 | 1937 | 0.02 | 94 | | | |
| 341 | 5.506 | 0.067 | 0.332 | 0.004 | 3.016 | 0.034 | 0.120 | 0.002 | 0.188 | 0.016 | 0.63 | 93 | 200 | 222 | 0.90 | 1846 | 0.01 | 1902 | 0.01 | 1963 | 0.02 | 94 | | | |
| 61 | 5.446 | 0.085 | 0.332 | 0.004 | 3.013 | 0.032 | 0.119 | 0.002 | 0.095 | 0.029 | 0.00 | 122 | 93 | 287 | 0.33 | 1848 | 0.01 | 1892 | 0.01 | 1941 | 0.02 | 95 | | | |
| 211 | 5.635 | 0.121 | 0.339 | 0.004 | 2.952 | 0.033 | 0.121 | 0.002 | 0.120 | 0.017 | 0.39 | 126 | 268 | 371 | 0.72 | 1880 | 0.01 | 1921 | 0.01 | 1966 | 0.02 | 95 | | | |
| 91 | 5.768 | 0.091 | 0.341 | 0.004 | 2.991 | 0.035 | 0.123 | 0.002 | 0.181 | 0.009 | 0.22 | 91 | 203 | 215 | 0.95 | 1893 | 0.01 | 1942 | 0.01 | 1994 | 0.02 | 97 | | | |
| 21 | 5.600 | 0.081 | 0.341 | 0.003 | 2.929 | 0.029 | 0.119 | 0.002 | 0.110 | 0.007 | 0.73 | 98 | 122 | 277 | 0.44 | 1894 | 0.01 | 1916 | 0.01 | 1941 | 0.02 | 97 | | | |
| 131 | 5.811 | 0.090 | 0.344 | 0.004 | 2.911 | 0.035 | 0.123 | 0.002 | 0.129 | 0.009 | 0.05 | 108 | 140 | 271 | 0.52 | 1903 | 0.02 | 1948 | 0.01 | 1996 | 0.02 | 95 | | | |
| 261 | 5.884 | 0.132 | 0.352 | 0.003 | 2.844 | 0.028 | 0.121 | 0.002 | 0.101 | 0.018 | 0.40 | 80 | 89 | 188 | 0.47 | 1921 | 0.01 | 1959 | 0.01 | 1999 | 0.02 | 96 | | | |
| 361 | 5.874 | 0.107 | 0.352 | 0.004 | 2.880 | 0.032 | 0.123 | 0.002 | 0.129 | 0.010 | 0.11 | 142 | 188 | 377 | 0.49 | 1942 | 0.01 | 1957 | 0.01 | 2025 | 0.02 | 98 | | | |
| 201 | 6.180 | 0.084 | 0.359 | 0.004 | 2.782 | 0.028 | 0.125 | 0.002 | 0.105 | 0.016 | 0.13 | 82 | 121 | 246 | 0.50 | 1979 | 0.01 | 2002 | 0.01 | 2025 | 0.02 | 97 | | | |
| 111 | 6.139 | 0.083 | 0.361 | 0.004 | 2.774 | 0.027 | 0.124 | 0.002 | 0.121 | 0.035 | 0.34 | 103 | 4 | 183 | 0.40 | 1985 | 0.01 | 1996 | 0.01 | 2007 | 0.02 | 98 | | | |
| 11 | 6.107 | 0.089 | 0.363 | 0.004 | 2.758 | 0.028 | 0.122 | 0.002 | 0.110 | 0.002 | 0.11 | 90 | 82 | 212 | 0.39 | 1994 | 0.01 | 1991 | 0.01 | 1988 | 0.02 | 100 | | | |
| 271 | 6.246 | 0.132 | 0.363 | 0.004 | 2.757 | 0.031 | 0.125 | 0.002 | 0.196 | 0.023 | 0.89 | 125 | 366 | 460 | 0.50 | 1995 | 0.01 | 2011 | 0.01 | 2028 | 0.02 | 101 | | | |
| 301 | 6.215 | 0.104 | 0.369 | 0.004 | 2.709 | 0.030 | 0.122 | 0.002 | 0.113 | 0.009 | 0.00 | 93 | 78 | 217 | 0.36 | 2026 | 0.02 | 2007 | 0.01 | 1987 | 0.02 | 101 | | | |
| 281 | 6.374 | 0.104 | 0.369 | 0.004 | 2.708 | 0.029 | 0.125 | 0.002 | 0.142 | 0.038 | 0.73 | 62 | 194 | 149 | 1.31 | 2026 | 0.01 | 2029 | 0.01 | 2031 | 0.02 | 99 | | | |
| 331 | 6.312 | 0.105 | 0.370 | 0.004 | 2.701 | 0.030 | 0.124 | 0.002 | 0.134 | 0.007 | 0.20 | 102 | 155 | 249 | 0.63 | 2030 | 0.02 | 2020 | 0.01 | 2010 | 0.02 | 101 | | | |
| 161 | 6.294 | 0.095 | 0.371 | 0.004 | 2.696 | 0.026 | 0.123 | 0.002 | 0.141 | 0.015 | 0.19 | 123 | 124 | 311 | 1.05 | 2034 | 0.01 | 2018 | 0.01 | 2001 | 0.02 | 101 | | | |
| 321 | 6.379 | 0.111 | 0.372 | 0.004 | 2.690 | 0.031 | 0.124 | 0.002 | 0.243 | 0.020 | 0.08 | 103 | 244 | 232 | 1.05 | 2038 | 0.02 | 2029 | 0.01 | 2021 | 0.02 | 100 | | | |
| 251 | 6.451 | 0.140 | 0.374 | 0.004 | 2.674 | 0.029 | 0.125 | 0.002 | 0.140 | 0.054 | 0.60 | 74 | 205 | 165 | 1.24 | 2048 | 0.01 | 2039 | 0.01 | 2031 | 0.03 | 100 | | | |
| 351 | 6.551 | 0.132 | 0.376 | 0.004 | 2.661 | 0.028 | 0.126 | 0.002 | 0.132 | 0.055 | 0.00 | 71 | 30 | 165 | 0.18 | 2057 | 0.01 | 2053 | 0.01 | 2049 | 0.03 | 100 | | | |
| 51 | 6.360 | 0.089 | 0.378 | 0.004 | 2.644 | 0.026 | 0.122 | 0.002 | 0.107 | 0.005 | 0.59 | 101 | 98 | 287 | 0.34 | 2068 | 0.01 | 2027 | 0.01 | 1985 | 0.02 | 104 | | | |
| 221 | 6.413 | 0.137 | 0.379 | 0.004 | 2.640 | 0.029 | 0.123 | 0.002 | 0.131 | 0.024 | 0.25 | 43 | 67 | 138 | 0.49 | 2071 | 0.01 | 2034 | 0.01 | 1987 | 0.02 | 103 | | | |
| 191 | 6.496 | 0.097 | 0.380 | 0.004 | 2.635 | 0.025 | 0.124 | 0.002 | 0.108 | 0.009 | 0.21 | 94 | 96 | 219 | 0.44 | 2074 | 0.01 | 2045 | 0.01 | 2017 | 0.02 | 102 | | | |
| 81 | 6.536 | 0.100 | 0.382 | 0.004 | 2.631 | 0.031 | 0.125 | 0.002 | 0.108 | 0.005 | 0.11 | 72 | 62 | 183 | 0.44 | 2077 | 0.02 | 2051 | 0.01 | 2025 | 0.02 | 102 | | | |
| 151 | 6.524 | 0.107 | 0.382 | 0.004 | 2.621 | 0.026 | 0.124 | 0.002 | 0.138 | 0.014 | 0.00 | 122 | 133 | 281 | 0.47 | 2084 | 0.01 | 2049 | 0.01 | 2015 | 0.02 | 103 | | | |
| 311 | 6.333 | 0.100 | 0.382 | 0.004 | 2.615 | 0.029 | 0.124 | 0.002 | 0.069 | 0.016 | 0.00 | 72 | 83 | 179 | 0.47 | 2088 | 0.02 | 2050 | 0.01 | 2013 | 0.02 | 103 | | | |
| 101 | 6.570 | 0.102 | 0.383 | 0.005 | 2.611 | 0.031 | 0.124 | 0.002 | 0.097 | 0.002 | 0.08 | 118 | 102 | 289 | 0.38 | 2090 | 0.02 | 2055 | 0.01 | 2020 | 0.02 | 103 | | | |
| 31 | 6.690 | 0.092 | 0.383 | 0.004 | 2.545 | 0.024 | 0.124 | 0.002 | 0.959 | 0.003 | 0.21 | 97 | 173 | 222 | 0.75 | 2136 | 0.01 | 2071 | 0.01 | 2007 | 0.02 | 106 | | | |
| 41 | 6.813 | 0.091 | 0.396 | 0.004 | 2.527 | 0.024 | 0.125 | 0.002 | 0.117 | 0.033 | 1.44 | 101 | 150 | 280 | 0.54 | 2149 | 0.01 | 2087 | 0.01 | 2027 | 0.02 | 106 | | | |

Table II

Textural features of zircon grains from the studied samples and interpretation.

| sample | External shape | Core texture | Main core texture | Recrystallisation/ Replacement | Overgrowth | Transgressive fronts and patches | Fractures and inclusions | Metamictization (%) | Ages | Th / U |
|---------------|--|--|--|--|--|--|---|---|--|--|
| CNP13F | Elongated (5:1), pale brown, round to subhedral | Patchy, convolute, non- luminescent; inner dark CL seam; outer bright CL seam | Highly resorbed, dark-CL; blurred "ghost" OZP; pyramidal sections w/ sector zoning | Broadening of oscillatory bands; darkening of wider bands | Homogeneous medium grey CL | Convolute/patchy cores, void infilling; round CL-bright unzoned patches | Healed fractures | 30% of zircons (black cauliflower) | Core: 3.3 Ga; rim: 2.8 Ga | Overdispersed |
| CNP77 | Stubby (2:1) and round, rough surface, fractured (subhedral); zircon mixture | Inherited resorbed patchy dark inner cores (25%) | 1. broadened OZP zoning. 2. bright cloudy crystallisation | Dark overgrowth. Transgressive fuzzy zoned or unzoned recrystallisa- tion | Dark-CL fuzzy sector zoning pattern; planar growth banding | Highly resorbed convolute pattern, void in-filling, transgressive fronts | Very fractured; Non- luminescent healed- fractures (50%) | Non-luminescent cataclastic elongated zircons (40%); cauliflowers (10%) | Core1: 3.3-3.0 Ga; rim1: 2.7 Ga; core2: 2.0-1.8 Ga; rim2? | Overdispersed 2 trends (< 0.1) |
| Mi21 | Subhedral to anhedral (round) (2:1), smooth surface; very fractured | Core 1: Inherited dark CL OZP and internal transgressive bulging; completely resorbed non- luminescent roots. | Core 2: Original euhedral medium-grey CL oscillatory pattern zoning. | Broadening of OZP; dark CL thickened sectors; some overgrowth controlled by healed fractures | Planar / convolute growth banding; fir- tree and radial sector zoning patterns | CL-bright transgressive fronts through "ghost" OZP (internal and outer cores) | Fractured; healed- fractures and composite zircons | Not observed | Core 2: 3.1 Ga; CL- bright unzoned growth rim: 2.2 Ga | Overdispersed |
| Mi30 | Subhedral (round); aspect ratio 2:1; rough borders; fractured | The CL-dark ho- mogeneous inner core | Original euhedral OZP (core 2) affected by sector zoning recrystallisation (60%), broadened in the centre. | Bright luminescent overgrowth (transgressive over inherited structures) | Transgressive planar growth banding (dominant); fir-tree sector zoning new overgrowth | Transgressive fronts affecting the sector zoning | Recrystallisation after fracturing; healed- fractures | Very few non- luminescent inner cores (metamict) | Core 2: 3.0 Ga; sector zoning: 1.9 Ga? 2. outer rim: 1.77 Ga | Magmatic (0.1 - 1.0) |
| Mi14 | Euhedral. Aspect ratio 3:1; mostly fractured; very rough borders; annealed metamict | CL-dark patchy or convolute inner core (20%) very resorbed | Almost totally annealed (polygonal) zircon; some preserve OZP but broaden; Smooth core surface; distinct core and rim | Planar sector zoning recrystallisa- tion | New growth zone: dark CL homoge- neous | Hydrothermal recrystallisation; leaching fluids | Healed fractures; altered fractures (metamict infilling) | Abundant in the inner cores | Core: 2.95 Ga; sector zoning + an- nealing: 2.0 Ga | 2 trends (0.1-1.0) - (0.2-0.4) |
| Mi19B | Subhedral to round; aspect ratio 2:1 | Inherited magmatic zircons (2.04 Ga) | a blurred magmatic broadening of bands. | Sector zoning recrystallisa- tion. | Medium-grey CL planar zoning. | CL-bright concordant front. | α -decay damage cracks | Material loss on fractures | Inherited: 2.0 Ga; sector zoning: 46 \pm 44 Ma | 1 trend (0.4-1.0) |

Table III
Supplementary database of U-Pb geochronological results for the Nico Pérez Terrane (including the Rivera block).

| # | sample | Latitude | Longitude | Age (Ma) | 2 σ | Rock-type | Unit | Method | Interpretation | Reference |
|----|-------------------|---------------|---------------|----------|------------|-----------------------|---------------------------------------|-------------------------|----------------|-----------------------------|
| 1 | 27-G-35 | 34°32'S | 55°15'W | 630 | n.d. | phyllite | Lavalleye Group | U-Pb rutile | metamorphic | Sánchez-Bettucci et al. [6] |
| 2 | 6198 | 34°21'04"S | 55°07'43"W | 1735 | +32/-17 | gneiss | Campanero Complex | U-Pb conv zircon | magmatic | Sánchez-Bettucci et al. [6] |
| 3 | 8-9 | 33°30'39.10"S | 55°12'2.51"W | 1760 | 3.3 | Rapakivi granite | Illescas Granite | Rb-Sr (WR) isochrone | magmatic | Umpierre & Halpern (1971) |
| 4 | AA-12 | 33°13'34.13"S | 55°31'29.15"W | 602 | 4.2 | granitic mylonite | Sarandí del Yí Shear Zone | U-Pb LA-ICP-MS titanite | cooling age | Oriolo et al. (2016b) |
| 5 | AA-13 | 33°16'11.16"S | 55°33'51.56"W | 588 | 7.1 | granitic mylonite | Sarandí del Yí Shear Zone | U-Pb LA-ICP-MS titanite | cooling age | Oriolo et al. (2016b) |
| 6 | AC-104 (cores) | 34°17'36.37"S | 54°25'5.57"W | 778 | 7 | Mafic migmatite | Cerro Olivo Complex | U-Pb SHRIMP zircon | magmatic | Masquelin et al. [7] |
| 7 | AC-104 (rims) | 34°17'36.37"S | 54°25'5.57"W | 637 | 11 | Mafic migmatite | Cerro Olivo Complex | U-Pb SHRIMP zircon | metamorphic | Masquelin et al. [7] |
| 8 | AC-133b | 34°20'14.08"S | 54°25'38.66"W | 794 | 8 | Felsic orthogneiss | Cerro Olivo Complex | U-Pb SHRIMP zircon | magmatic | Lenz et al. [8] |
| 9 | AC-137b (cores) | 34°19'34.29"S | 54°25'9.44"W | 793 | 4 | Tonalitic gneiss | Cerro Olivo Complex | U-Pb SHRIMP zircon | magmatic | Lenz et al. [8] |
| 10 | AC-137b (rims) | 34°19'34.29"S | 54°25'9.44"W | 670 | 12 | Tonalitic gneiss | Cerro Olivo Complex | U-Pb SHRIMP zircon | metamorphic | Lenz et al. [8] |
| 11 | AC-166 | 34°21'17.00"S | 54°26'57.41"W | 546 | 7 | Porphyritic granite | El Pintor Granite | U-Pb ID TIMS | magmatic | Masquelin [9] |
| 12 | AC-167 (cores) | 34°16'42.3"S | 54°23'46.6"W | 990 | - | Kfs-augen migmatite | Cerro Olivo Complex | U-Pb SHRIMP zircon | inherited | Masquelin et al. [7] |
| 13 | AC-296m (cores) | 34°18'54.24"S | 54°23'53.72"W | 796 | 8 | Mafic granulite | Cerro Olivo Complex | U-Pb SHRIMP zircon | magmatic | Lenz et al. [8] |
| 14 | AC-296m (rims) | 34°18'54.24"S | 54°23'53.72"W | 649 | 4 | Mafic granulite | Cerro Olivo Complex | U-Pb SHRIMP zircon | metamorphic | Lenz et al. [8] |
| 15 | AC-301 | 34°20'42.2"S | 54°23'56.1"W | 626 | 25 | Felsic migmatite | Cerro Olivo Complex | U-Pb SHRIMP zircon | metamorphic | Masquelin et al. [7] |
| 16 | AC-338a | 34°18'23.80"S | 54°24'25.87"W | 802 | 12 | Tonalitic gneiss | Cerro Olivo Complex | U-Pb SHRIMP zircon | magmatic | Lenz et al. [8] |
| 17 | AC-370a | 34°24'5.13"S | 54°24'33"W | 780 | 5 | Felsic migmatite | Cerro Olivo Complex | U-Pb SHRIMP zircon | magmatic | Lenz et al. [8] |
| 18 | AC-373b | 34°20'29.80"S | 54°24'3.35"W | 795 | 8 | Mafic granulite | Cerro Olivo Complex | U-Pb SHRIMP zircon | magmatic | Lenz et al. [8] |
| 19 | BRAF-212 | 34°27'47.66"S | 55°10'3.68"W | 1429 | 21 | Rhyolite | Zanja del Tigre Complex | U-Pb ID-TIMS zircon | magmatic | Oyhantcabal et al. (2005) |
| 20 | BRAF-213 | 34°28'59.27"S | 55°12'39.17"W | 1492 | 4 | Metagabbro | Zanja del Tigre Complex | U-Pb ID-TIMS zircon | magmatic | Oyhantcabal et al. (2005) |
| 21 | BUY-54-11 | 31°38'11.11"S | 55°22'5.41"W | 2095 | 15 | Mafic granulite | Valentines- Rivera Granulitic Complex | U-Pb LA-ICP-MS zircon | magmatic | Oriolo et al. (2016a) |
| 22 | BUY-57-11 (cores) | 31°41'18.30"S | 55°16'13.60"W | 2087 | 7 | Tonalitic gneiss | Valentines- Rivera Granulitic Complex | U-Pb LA-ICP-MS zircon | magmatic | Oriolo et al. (2016a) |
| 23 | BUY-57-11 (rims) | 31°41'18.30"S | 55°16'13.60"W | 1857 | 45 | Tonalitic gneiss | Valentines-Rivera Granulitic Complex | U-Pb LA-ICP-MS zircon | metamorphic | Oriolo et al. (2016a) |
| 24 | BUY-61-11 | 31°44'52.40"S | 54°56'51.46"W | 2069 | 16 | Leucocratic gneiss | Valentines- Rivera Granulitic Complex | U-Pb LA-ICP-MS zircon | magmatic | Oriolo et al. (2016a) |
| 25 | BUY-63-11 | 31°39'12"S | 54°54'11"W | 596 | 2 | Amarillo Granite | Neoproterozoic granitoids | U-Pb LA-ICP-MS zircon | magmatic | Oriolo et al. (2016a) |
| 26 | BUY-64-11 | 32°53'40.18"S | 54°48'58.26"W | 598 | 2.2 | granitic mylonite | Sierra de Sosa Shear Zone | Ar-Ar hornblende | cooling age | Oriolo et al. (2016a) |
| 27 | BUY-65-11 | 33°2'4.35"S | 55°3'53.82"W | 2106 | 21 | Felsic granulite | Cerro Chato block | U-Pb LA-ICP-MS zircon | magmatic | Oriolo et al. (2016a) |
| 28 | BUY-66-11 | 32°50'40.69"S | 54°44'7.47"W | 549 | 2.9 | granitic mylonite | Tupambala Shear Zone | U-Pb LA-ICP-MS zircon | deformation | Oriolo et al. (2016b) |
| 29 | BUY-77-11 | 33°30'28"S | 54°56'45"W | 610 | 2 | Zapicán diorite | Neoproterozoic granitoids | U-Pb LA-ICP-MS zircon | magmatic | Oriolo et al. (2016ab) |
| 30 | BUY-88-11 | 33°57'37.90"S | 55°38'50.37"W | 2078 | 4.7 | granite | Cerro Colorado Granite | U-Pb LA-ICP-MS zircon | magmatic | Oriolo et al. (2016b) |
| 31 | CH-174 | 34°14'35.57"S | 54°16'59.87"W | 786 | 9 | Felsic orthogneiss | Cerro Bori Orthogneisses | U-Pb SHRIMP zircon | magmatic | Lenz et al. [8] |
| 32 | CH-33a | 34°17'19.72"S | 54°11'4.51"W | 767 | 9 | Mafic granulite | Chafalote Paragneisses | U-Pb SHRIMP zircon | magmatic | Lenz et al. [8] |
| 33 | CH-43d | 34°17'40.27"S | 54°10'55.11"W | 772-765? | - | Mafic granulite | Chafalote Paragneisses | U-Pb SHRIMP zircon | magmatic | Lenz et al. [8] |
| 34 | COR-42 | 34°24'42.40"S | 54°25'11.56"W | 797 | 8 | Mylonitic orthogneiss | Cerro Bori Orthogneisses | U-Pb SHRIMP zircon | magmatic | Lenz et al. [8] |
| 35 | EP-210 (prov 3) | 32°32'18.38"S | 53°48'3.67"W | 1823-665 | - | psamo-pelitic schist | La Micaela Schists | U-Pb LA-ICP-MS zircon | detrital | Peel et al. [10] |
| 36 | EP-214 (prov 1) | 32°33'11.32"S | 53°48'37.31"W | 587.7 | 3.9 | Grt-chlorite schist | La Micaela Schists | U-Pb LA-ICP-MS zircon | detrital | Peel et al. [10] |
| 37 | EP-214 (prov 2) | 32°33'11.32"S | 53°48'37.31"W | 569.5 | 3.3 | Grt-chlorite schist | La Micaela Schists | U-Pb LA-ICP-MS zircon | detrital | Peel et al. [10] |
| 38 | EP-228 (cores) | 32°35'38.42"S | 53°49'44.77"W | 753.8 | 8.4 | anatectic paragneiss | Cerro Olivo Complex | U-Pb LA-ICP-MS zircon | detrital | Peel et al. [10] |
| 39 | EP-228 (rims) | 32°35'38.42"S | 53°49'44.77"W | 668 | 17 | anatectic paragneiss | Cerro Olivo Complex | U-Pb LA-ICP-MS zircon | metamorphic | Peel et al. [10] |
| 40 | FZ6 | 33°55'19.6"S | 54°48'59.8"W | 2787 | 6 | Granitic mylonite | Archean granitoids | U-Pb LA-ICP-MS zircon | magmatic | Gaucher et al. (2014) |
| 41 | G | 34°26'17.39"S | 55°12'38.59"W | 1203 | 65 | Metagabbro | Cañada del Espinillo | K-Ar (WR) | cooling age | Gomez Rivas [11] |

(continued on next page)

Table III (continued)

| # | sample | Latitude | Longitude | Age (Ma) | 2 σ | Rock-type | Unit | Method | Interpretation | Reference |
|----|------------------|----------------|---------------|-----------|------------|--------------------|-------------------------------|---------------------------|----------------|--------------------------------|
| 42 | Hart1 | 34°25'19"S | 54°14'25"W | 762 | 8 | gneiss | Cerro Olivo Complex | U-Pb SHRIMP zircon | magmatic | Hartmann et al. (2002) |
| 43 | Hart2 | 34°07'S | 55°12'17"W | 633 | 8 | monzogranite | Santa Lucía Granite | U-Pb SHRIMP zircon | magmatic | Hartmann et al. (2002) |
| 44 | Hart3 | 34°16'S | 54°07'W | 571 | 8 | dacite | Sierra de Aguirre Fm | U-Pb SHRIMP zircon | magmatic | Hartmann et al. (2002) |
| 45 | LAN-108 | 55°15'48.3"O | 55°15'48.3"O | 1433 | 6 | Metatuffs | Parque UTE Group | U-Pb LA-ICP-MS zircon | magmatic | Gaucher et al. (2011) |
| 46 | MAZ-59 | 33°49'24.64"S | 55°11'55.21"W | 610 | 3 | Granodiorite | Neoproterozoic granitoids | U-Pb LA-ICP-MS zircon | magmatic | Gaucher et al. (2014) |
| 47 | NP-154 | 34°35'51"S | 55°09'23"W | 1754 | 7 | Mylonitic granite | Campanero Unit | U-Pb SHRIMP zircon | magmatic | Mallmann et al. (2007) |
| 48 | PCH-0869 | 34°20'21.39"S | 54°24'17.74"W | 788 | 6 | Mafic granulite | Cerro Bori Orthogneisses | U-Pb SHRIMP zircon | magmatic | Lenz et al. [8] |
| 49 | SA-1 | 34°49'20"S | 55°14'49"W | 579 | 1.5 | syenite | Pan de Azúcar Syenite | Ar-Ar hornblende | cooling age | Oyhantcábal et al. [12] |
| 50 | sample 1 (core) | 33°32' 15.90"S | 54°55'37.45"W | 3404 | 8 | Metatonalite | La China Complex | U-Pb SHRIMP zircon | inherited | Hartmann et al. (2001) |
| 51 | sample 1 (rim) | 33°32' 15.90"S | 54°55'37.45"W | 2721 | 7 | Metatonalite | La China Complex | U-Pb SHRIMP zircon | metamorphic | Hartmann et al. (2001) |
| 52 | sample 3 (core) | 31°43'3.90"S | 55°22'30.51"W | 2140 | 6 | Meta-trondhjemite | Rivera Granulitic Complex | U-Pb SHRIMP zircon | magmatic | Santos et al. (2003) |
| 53 | sample 3 (rim) | 31°43'3.90"S | 55°22'30.51"W | 2077 | 6 | Meta-trondhjemite | Rivera Granulitic Complex | U-Pb SHRIMP zircon | metamorphic | Santos et al. (2003) |
| 54 | sample 4 (core) | 33°14'59"S | 55°13'29"W | 2163 | 22 | Granulite | Valentines Granulitic Complex | U-Pb SHRIMP zircon | magmatic | Santos et al. (2003) |
| 55 | sample 4 (rim) | 33°14'59"S | 55°13'29"W | 2058 | 3 | Granulite | Valentines Granulitic Complex | U-Pb SHRIMP zircon | metamorphic | Santos et al. (2003) |
| 56 | SB-050 | 34°50'35"S | 54°56'58"W | 564 | 7 | granite | Maldonado Granite | U-Pb SHRIMP zircon | magmatic | Oyhantcábal et al. (2009) |
| 57 | SB-632 | 34°35'24"S | 55°26'30"W | 584 | 13 | granite | Matazojo granitic complex | Pb-Pb titanite | magmatic | Oyhantcábal et al. (2007) |
| 58 | SH-5 | 34°31'12"S | 55°09'44"W | 627 | 23 | granodiorite | Neoproterozoic granitoids | U-Pb SHRIMP zircon | magmatic | Oyhantcábal et al. (2009) |
| 59 | SOL-3 | 34°01'44"S | 55°08'W | 583 | 7 | granodiorite | Mangacha Granite | U-Pb SIMS zircon | magmatic | Gaucher et al. (2008) |
| 60 | U13MH04 | 33°15'12.13"S | 54°43'44.45"W | 600.4 | 1.1 | quartz-micaschists | Las Tetás Complex | Ar-Ar muscovite | metamorphic | Oriolo et al. (2016b) |
| 61 | U13MH04 | 33°15'12.13"S | 54°43'44.45"W | 590 | 11 | quartz-micaschists | Las Tetás Complex | Rb-Sr mica + WR isochrone | cooling age | Oriolo et al. (2016b) |
| 62 | URPR-12 | 34°37'S | 54°51'W | 587 | 16 | granite | Aiguá Granite | U-Pb zircon | magmatic | Bassi et al. (2000) |
| 63 | URPR-4a | 34°34'S | 55°10'W | 572 | 14 | granite | Carapé Granite | U-Pb conv zircon | magmatic | Sánchez-Bettucci et al. (2003) |
| 64 | URPR-63 | 34°54'14"S | 55°14'13"W | 1737 | 5.7 | gneiss | Campanero Complex | U-Pb SHRIMP zircon | magmatic | Oyhantcábal et al. (2005) |
| 65 | URPR-68 | 34°29'58.34"S | 55°13'14.5"W | 3197-702 | - | Metasandstone | Fuente del Puma Fm | U-Pb SHRIMP zircon | derital | Oyhantcábal et al. (2005) |
| 66 | URPR-69 | 34°33'12.60"S | 55° 5'26.66"W | 3350-1780 | - | Metasandstone | Zanja del Tigre Complex | U-Pb SHRIMP zircon | derital | Oyhantcábal et al. (2005) |
| 67 | UY08-1 | 31°45'13.65"S | 55°11'24.92"W | 586 | 2.7 | syenogranite | Las Flores Granite | U-Pb SHRIMP zircon | magmatic | Oyhantcábal et al. (2012) |
| 68 | UY08-2 | 31°32'38.65"S | 55°29'43.93"W | 585 | 2.5 | syenogranite | Sobresaliente Granite | U-Pb SHRIMP zircon | magmatic | Oyhantcábal et al. (2012) |
| 69 | UY08-4a | 31°39'50"S | 55°10'17"W | 1920 | 18 | Mesocratic gneiss | Rivera Granulitic Complex | Th-U-Pb CHIME-EPMA mon | metamorphic | Oyhantcábal et al. (2012) |
| 70 | UY08-4a | 31°39'50"S | 55°10'17"W | 606 | 10 | Mylonite | Rivera Shear Zone | K-Ar muscovite | cooling age | Oyhantcábal et al. (2012) |
| 71 | UY08-5 | 31°41'29.69"S | 55°22'59.03"W | 1975 | 5 | Leucocratic gneiss | Rivera Granulitic Complex | Th-U-Pb CHIME-EPMA mon | metamorphic | Oyhantcábal et al. (2012) |
| 72 | UY08-8 | 31°34'35.67"S | 55°34'11.76"W | 1981 | 2 | Mesocratic gneiss | Rivera Granulitic Complex | Th-U-Pb CHIME-EPMA mon | metamorphic | Oyhantcábal et al. (2012) |
| 73 | UY08-8 | 31°34'35.67"S | 55°34'11.76"W | 2094 | 17 | Mesocratic gneiss | Rivera Granulitic Complex | Pb-Pb titanite | metamorphic | Oyhantcábal et al. (2012) |
| 74 | UY08-8 (1) | 31°34'35.67"S | 55°34'11.76"W | 2114 | 3.1 | Mesocratic gneiss | Rivera Granulitic Complex | U-Pb SHRIMP zircon | magmatic | Oyhantcábal et al. (2012) |
| 75 | UY08-8 (2) | 31°34'35.67"S | 55°34'11.76"W | 2147 | 8.7 | Mesocratic gneiss | Rivera Granulitic Complex | U-Pb SHRIMP zircon | magmatic | Oyhantcábal et al. (2012) |
| 76 | UY-10-05 (cores) | 32°28'45"S | 54°28'1.8"W | 776 | 12 | gneiss | Cerro Olivo Complex | U-Pb SHRIMP zircon | magmatic | Oyhantcábal et al. (2009) |
| 77 | UY-10-05 (rim) | 34°28'45"S | 54°28'2"W | 641 | 17 | gneiss | Cerro Olivo Complex | U-Pb SHRIMP zircon | metamorphic | Oyhantcábal et al. (2009) |
| 78 | UY-1-13 | 33°13'43.41"S | 54°43'3.76"W | 550.5 | 2.7 | marbles | Las Tetás Complex | Rb-Sr mica + WR isochrone | cooling age | Oriolo et al. (2016b) |
| 79 | UY-1-13 | 33°13'43.41"S | 54°43'3.76"W | 621.4 | 1 | marbles | Las Tetás Complex | Ar-Ar phlogopite | metamorphic | Oriolo et al. (2016b) |

(continued on next page)

Table III (continued)

| # | sample | Latitude | Longitude | Age (Ma) | 2σ | Rock-type | Unit | Method | Interpretation | Reference |
|----|------------|---------------|----------------|----------|-----|--------------------|--------------------------------------|-------------------------|----------------|---------------------------|
| 80 | UY-12-05 | 34°38'25"S | 55°17'23"W | 573 | 11 | pebbly sandstones | Barriga Negra Group | U-Pb SHRIMP zircon | magnetic | Oyhantcábal et al. (2009) |
| 81 | UY-13-14 | 34°53'19.06"S | 55° 2'27.31"W | 420 | - | granitic mylonite | Sierra Ballena Shear Zone | Ar-Ar amphibole | cooling age | Oriole et al. (2016b) |
| 82 | UY-26-14 | 34°17'49.97"S | 54°37'56.14"W | 5897 | 6.2 | Mylonitic granite | Florencia Granite | K-Ar muscovite | cooling age | Oriole et al. (2016b) |
| 83 | UY-2-A | 34°17'44.12"S | 54°32' 25"W | 771 | 6 | Mafic gneiss | Cerro Bort Orthogneisses | U-Pb SHRIMP zircon | magnetic | Leitz et al. (2011) |
| 84 | UY3-05 (1) | 31°41'17.43"S | 55°24'3.05"W | 2093 | 36 | Leucocratic gneiss | Valentines- Rivera Granulite Complex | U-Pb SHRIMP zircon | magnetic | Oyhantcábal et al. (2012) |
| 85 | UY3-05 (2) | 31°41'17.43"S | 55°24'3.05"W | 2172 | 8 | Leucocratic gneiss | Valentines- Rivera Granulite Complex | U-Pb SHRIMP zircon | magnetic | Oyhantcábal et al. (2012) |
| 86 | UY-3-13 | 33°13'42.76"S | 54°42' 1.02"W | 586.8 | 1.1 | Mylonitic gneiss | Maria Alhina Shear Zone | Ar-Ar plateau age (Mus) | cooling age | Oriole et al. (2016b) |
| 87 | UY-40-14 | 33° 9'28.63"S | 54°57'52.29"W | 600 | 14 | Mylonitic gneiss | La China Complex | Ar-Ar amphibole | cooling age | Oriole et al. (2016b) |
| 88 | UY-41-14 | 33° 8'25.17"S | 55°10'21.98"W | 604.9 | 6.3 | quartz-micaschists | Las Torres Complex | K-Ar muscovite | cooling age | Oriole et al. (2016b) |
| 89 | UY-45-14 | 33°12'58.26"S | 54°41'40.13"W | 619.4 | 8.5 | Mylonitic gneiss | Maria Alhina Orthogneiss | K-Ar muscovite | cooling age | Oriole et al. (2016b) |
| 90 | UY-48-14 | 32°48'31.20"S | 54°16' 12.88"W | 615.2 | 6.6 | Mylonitic gneiss | Cerro Amaro Shear Zone | K-Ar muscovite | cooling age | Oriole et al. (2016b) |
| 91 | UY-57-14 | 32°58'48.57"S | 54°37'20.76"W | 630.2 | 6.1 | Mylonitic gneiss | Isla Patrolla Shear Zone | Ar-Ar amphibole | cooling age | Oriole et al. (2016b) |
| 92 | UY-6-14 | 34°33'19.31"S | 54°43'24.77"W | 6327 | 4.1 | Mylonitic gneiss | Cordillera Shear Zone | K-Ar muscovite | cooling age | Oriole et al. (2016b) |
| 93 | UY-7-04 | 34°43'36.01"S | 55° 5'31.02"W | 564 | 4.1 | amphibolite | Campanero Unit | Ar-Ar hornblende | cooling age | Oyhantcábal et al. (2009) |
| 94 | UY-8-05 | 34°20'30"S | 54°34'32"W | 614 | 3.2 | granite | Valdiva Granite Complex | Pb-Pb titanite | magnetic | Oyhantcábal et al. (2007) |
| 95 | ZAP-20 | 33°33'34"S | 54°55'24"W | 3096 | 45 | Migmatite | La China Complex | U-Pb LA-ICP-MS zircon | magnetic | Gaucher et al. (2011) |
| 96 | BDX-801-11 | 33°27'11.87"S | 55°18'44.90"W | 1768 | 11 | Rapakivi granite | Paleoproterozoic gneissoids | U-Pb LA-ICP-MS zircon | magnetic | Oriole et al. (2019) |
| 97 | UC-10 | 34°26'17.39"S | 55°12'38.59"W | 1479 | 4 | Metagabbro | Zanja del Tigre Complex | U-Pb LA-ICP-MS zircon | magnetic | Oriole et al. (2019) |
| 98 | UC-11 | 34°28'59.27"S | 55°12'39.17"W | 1482 | 6 | Metagabbro | Zanja del Tigre Complex | U-Pb LA-ICP-MS zircon | magnetic | Oriole et al. (2019) |

3. Experimental Design, Materials and Methods

3.1. Sample preparation

The sample preparation comprises the crushing and sieving of rock samples and fine grinding of the resulting products in the standard grain size of zircon ($50 < \Phi < 300$ microns) and then the separation concentration zircons. The mineral separation laboratory carried out these procedures at the Geochronological Research Center of the Universidade de São Paulo (CPGeo-IGc / USP). The heavy mineral concentrate was obtained using a Wilfley gravitational table, heavy liquids and magnetic separation by hand magnet and Frantz magnetic separator. The resulting impure zircon concentrates were cleaned from their gangue with ultrasound and strong acids, and the concentrated residual fraction was manually trickled under a binocular microscope (BM) by hand-picking. The separated zircons were placed in mounts on epoxy resin. Standard protocols to place grains in the epoxy resin plate were followed. After observation under BM, the resin plate was super-polished to expose the central part of the grains and metallised to be observed by cathodoluminescence in the SEM.

3.2. Optical binocular microscope

The first step in microscopic analysis of zircons is to study them in a Petri dish with ethanol, under a high-resolution binocular microscope, and select and document the grains by photomicrographs. Properties such as colour, degree of transparency, external morphology and crystalline development are observed. The main external characteristics to pick up are (i) length to width aspect ratios, (ii) colour and degree of transparency, (iii) presence of xenocryst cores and inclusions of other minerals, (iv) degree of fracturing and alteration, and (v) crystallographic typology, like the relationship between prismatic vertical axes and pyramidal crystal faces.

3.3. Cathodoluminescence and textural study

Once the zircon mount was made in epoxy resin, the grains are numbered first with the transmission microscope (40x). The mount is placed on the excimer laser microprobe, in which a 15 kV electron beam bombardment generates cathodoluminescence (CL) images. CL imaging is essential to describe textural patterns. Zircon morphology and texture reflect the geological history, especially in magmatic nucleation, overgrowing and metamorphic recrystallisation, deformation, or volume change, and chemical alteration [2].

3.4. LA-ICP-MS U-Pb analytical technique

We set up the isotopic data and zircon dating at the Geochronological Laboratory of the Geosciences Institute from the University of São Paulo (Brazil). The LA-ICP-MS equipment locates at the CPGeo-IGc/USP and has an excimer laser of ArF gas (193 nm) coupled to the Neptune™ High-Resolution Multi-collector ICP-MS. The excimer laser used here provides a better regularity of abrasion, reducing the fractionation between masses due to its high optical quality and source stability [3]. The ICP-MS analytical procedure calibrates using the international standard zircon Temora-1 standard zircon ($^{206}\text{Pb}/^{238}\text{U} = 0.06683$). Results are displayed in $^{206}\text{Pb}/^{238}\text{U}$ vs $^{207}\text{Pb}/^{235}\text{U}$ Wetherill's Concordia diagram and $^{206}\text{Pb}/^{238}\text{U}$ vs $^{207}\text{Pb}/^{206}\text{Pb}$ Tera-Wasserburg's graph, using IsoplotR [4]. Wetherill's Concordia diagrams served both to model magmatic pro-toliths' concordant age and the systematic radiogenic lead loss due to subsequent geological processes. The zircons were ablated during 40 seconds in the 193 nm Excimer Laser Ablation

System, at 7–6 Hz, 6mJ and full energy, obtaining spots of ca. 25 μm (Helium: MFC1 = 0.300 L/min, MFC2 = 0.300 L/min, Argon: Aux.= 0.95 L/min, sample = 0.978 L/min).

4. Figures and Tables

4.1. Petrographic data

The petrographic data corresponding to section 1 is commented on the following captions and documented on the photographic and photo-micrographic plates (Figs. 2–8).

4.2. U-Pb Isotopic data of zircons

Table I contains the isotopic results obtained in the U-Pb Geochronology Laboratory of the University of Sao Paulo between 2016 and 2017 from two sample sets. It contains the isotopic ratios of U and Pb commonly used to calculate the absolute ages $T^{238\text{U}/206\text{Pb}}$, $T^{235\text{U}/207\text{Pb}}$ and $T^{207/206\text{Pb}}$. There are the results of concordant and isochronal ages of radiogenic Pb loss for the six dated samples in the last column. Although the results of the isotopic ratios present uncertainties obtained at one sigma, the calculations of the ages with the Vermeesch's Isoplot-R software [4] were calculated at two sigmas.

Table II contains a comparative analysis of the different internal textures of the dated zircons from each of the six samples in this study. The items considered for the correlation were the external morphological aspects, the internal texture subdivision in (i) core, (ii) rim, and (iii) other diagnostic features due to the crystallisation/recrystallisation of the grains. We consider it a priority to evaluate the presence of overgrowth, transgressive replacement fronts, inclusions, fracturing, and alteration linked to the damage caused by radiation. The Th/U ratio was also evaluated. All the samples except one presented inheritance of Archean ages.

Table III compilation of antecedents related to absolute ages by the U-Pb method in zircon from the central-eastern and south-eastern region of Uruguay. It is an exhaustive list of antecedents to date, understanding that the rapid evolution of geochronological knowledge in this region requires a continuous review of published data. Although the list refers exclusively to the U-Pb data, a single Rb-Sr isochronal age antecedent (corresponding to the Umpierre & Halpern's document of 1971) was included and considered a valuable antecedent for the dating of the "Illescas Granite". The advantage of this table is that it presents the Latitude - Longitude coordinates collected and recalculated from the consulted works.

4.3. Supplementary data

Table III

Ethics Statement

- This material is the authors' original work, which has not been previously published elsewhere.
- The authors did not submit this paper for other publication elsewhere.
- The paper reflects the authors' research and analysis wholly and truthfully.
- The paper properly credits the meaningful contributions of co-authors and co-researchers.
- The results are appropriately placed in the context of prior and existing research.
- All sources used are correctly disclosed (correct citation).

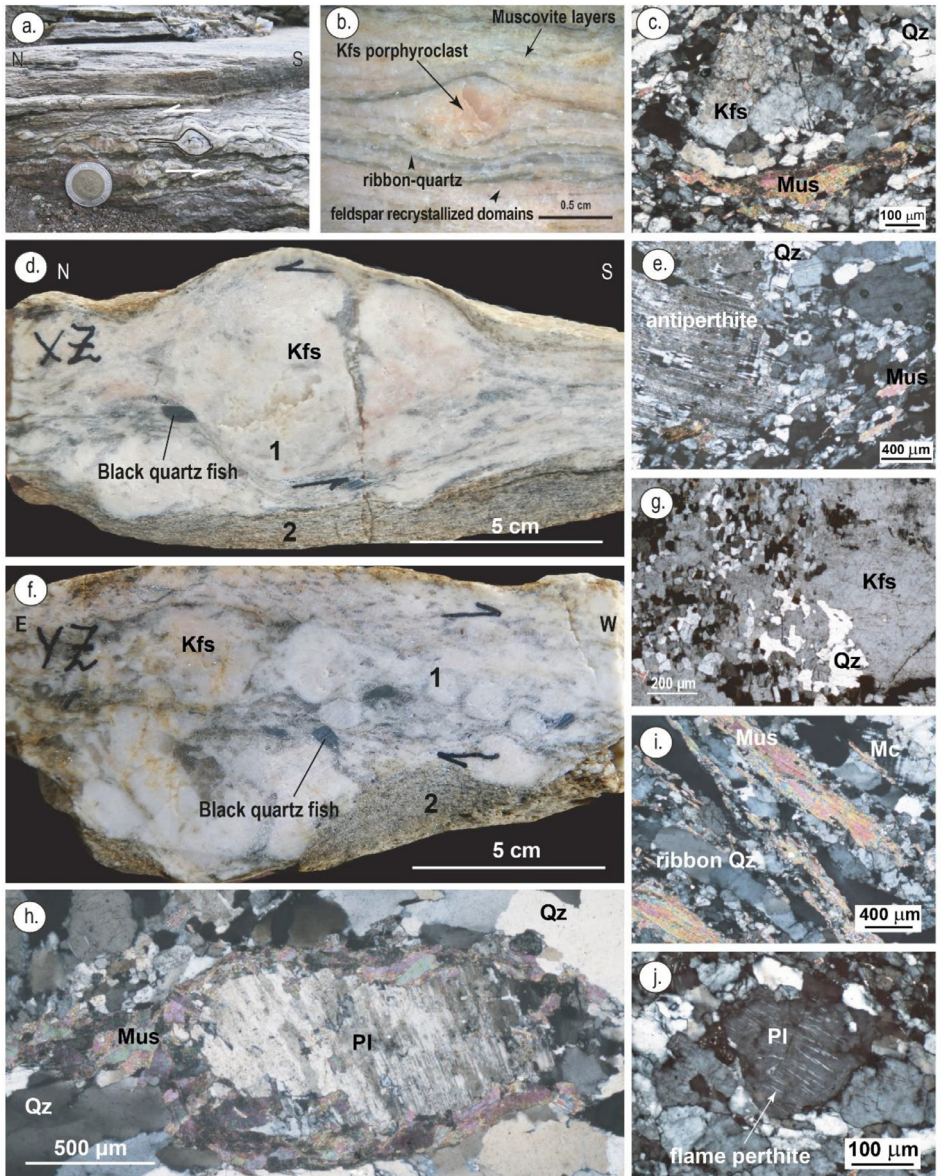


Fig. 8. Flat-lying muscovite augen gneiss (Mi06) in the “Zapican Thrust”, a) Mylonitic foliation (coin is 2.5 cm). b) K-feldspar porphyroblast. c) Phenocryst vs matrix. d) Section in XZ plane and sinistral shear. e) Phenocryst of patchy antiperthitic plagioclase. f) Section in YZ plane and dextral shear. g) Partial recrystallisation of Kfs phenocryst. h) Antiperthitic porphyroblast surrounded by muscovite. i) Detail of muscovite layers and ribbon quartz. j) Flame perthite in plagioclase.

- All authors have been personally and actively involved in substantial work leading to the paper and will take public responsibility for its content.
- No information obtained for experimentation with human subjects was used.
- No information obtained for experimentation with animals was used.

CRedit Author Statement

Henri Masquelin: Conceptualisation, Methodology, Software, writing-original draft preparation; **Tahar Aífa:** Data curation, Software, Writing - original draft preparation; **Fernando Scaglia:** Visualization, Investigation; **Miguel Basei:** Data curation, software, Validation.

Declaration of Competing Interest

The authors declare that they have no known competing financial interests or personal relationships which have or could be perceived to have influenced the work reported in this article.

Acknowledgments

We are indebted to the Director Lic. Nestor Campal authorised the use of the airborne geophysical data of DINAMIGE for academic purposes. We also thank Bruna Sanches, Nairé Gabriel, and the rest of the team at the Centro de Pesquisas Geocronológicas of the University of São Paulo. We thank Dr Elena Peel for the help regarding the use of standard deviation in the Concordia diagram. The authors are grateful to CSIC (UdelaR) for the funding granted (first author's project CSIC-2015 C-604) and to the Faculty of Sciences of the [Universidad de la República](#) (Uruguay) for the Logistics. They also acknowledge PEDECIBA - Geosciences, who provided third author's grants. To Ecos-sud Conicyt program n°U17U01 for funding the travels and per diem to Tahar Aífa and Henri Masquelin through a cooperation exchange program between the Rennes 1 and UdelaR universities since 2018. This work is also a contribution to the Unesco-igcp638 program.

References

- [1] C.W. Passchier, R.A. Trouw, *Microtectonics*, Springer Science & Business Media, 2005.
- [2] M.J. Kohn, N.M. Kelly, Petrology, and geochronology of metamorphic zircon, In Moser et al. (eds.), chapter 2, *Microstructural geochronology: Planetary records down to atom scale*, Geophysical Monograph Series, AGU, 2018, 35–61.
- [3] K. Sato, M.A.S. Basei, O. Siga Júnior, W.M. Sprousser, A.T. Onoe, Excimer laser (193 nm) acoplado ao ICP-MS Neptune: primeiros resultados de análises isotópicas, in: *Simpósio 45 Anos de Geocronologia no Brasil*, Resumos Expandidos, 2009, pp. 131–133. USP.
- [4] P. Vermeesch, IsoplotR: a free and open toolbox for geochronology, *Geosci. Front.* 9 (5) (2018) 1479–1493.
- [5] D.L. Whitney, B.W. Evans, Abbreviations for names of rock-forming minerals, *Am. Mineralogist* 95 (1) (2010) 185–187.
- [6] L. Sánchez Bettucci, F. Preciozzi, M.A.S. Basei, P. Oyhantçabal, E. Peel, J. Loureiro, Campanero Unit: a probable Paleoproterozoic basement and its correlation to other units of south-eastern Uruguay, in: *IV South American Symposium on Isotope Geology*, Short Papers, CBPM: IRD, Salvador, 2003, pp. 673–674.
- [7] H. Masquelin, L.A. D'Ávila Fernandes, C. Lenz, C.C. Porcher, N.J. McNaughton, The Cerro Olivo complex: a pre-collisional Neoproterozoic magmatic arc in Eastern Uruguay, *Int. Geol. Rev.* 54 (10) (2012) 1161–1183.
- [8] C. Lenz, L.A.D. Fernandes, N.J. McNaughton, C.C. Porcher, H. Masquelin, U–Pb SHRIMP ages for the Cerro Bori Orthogneisses, Dom Feliciano Belt in Uruguay: evidence of a ca. 800 Ma magmatic and ca. 650 Ma metamorphic event, *Precambrian Res.* 185 (3–4) (2011) 149–163.
- [9] H. Masquelin, in: *Evolução estrutural e metamórfica do Complexo Gnáissico Cerro Olivo, Sudeste do Uruguay*, Tese de Doutorado, CPGeo - UFRGS, 2002, pp. 1–344. 1 map.
- [10] E. Peel, L.S. Bettucci, M.A.S. Basei, Geology and geochronology of Paso del Dragón Complex (north-eastern Uruguay): implications on the evolution of the Dom Feliciano Belt (Western Gondwana), *J. South Am. Earth Sci.* 85 (2018) 250–262.
- [11] C. Gómez Rifas, in: *A zona de cisalhamento sinistral de Sierra Ballena no Uruguai*, Tese de doutorado, IG-USP, São Paulo, 1995, pp. 1–243. 5 maps.
- [12] P. Oyhantçabal, S. Siegesmund, K. Wemmer, S. Presnyakov, P. Layer, Geochronological constraints on the evolution of the southern Dom Feliciano Belt (Uruguay), *J. Geol. Soc.* 166 (6) (2009) 1075–1084.